

inelastic Neutrino Scattering

Arie Bodek

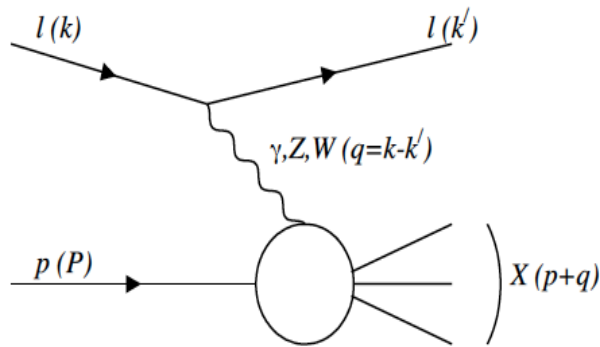
University of Rochester

December 2013

**Modeling Inelastic Low Energy Neutrino Scattering on Nuclear Targets
at all values of Q^2**

Past, Present and Future

Neutrino Cross sections



In electron and neutrino scattering we categorize cross sections by the mass of the final state hadronic system : W

$W = M = 0.938 \text{ GeV}$ -> elastic (free nucleons). quasielastic scattering (nuclei)

$1.1 < W < 1.9$ Inelastic scattering in the resonance region

$W > 1.9 \text{ GeV}$ Inelastic scattering in the continuum

$$W^2 = (p+q)^2 = M^2 + 2M\nu - Q^2$$

ν = energy transfer to target

$y = \nu / E$ = inelasticity

Q^2 = square of the four momentum transfer

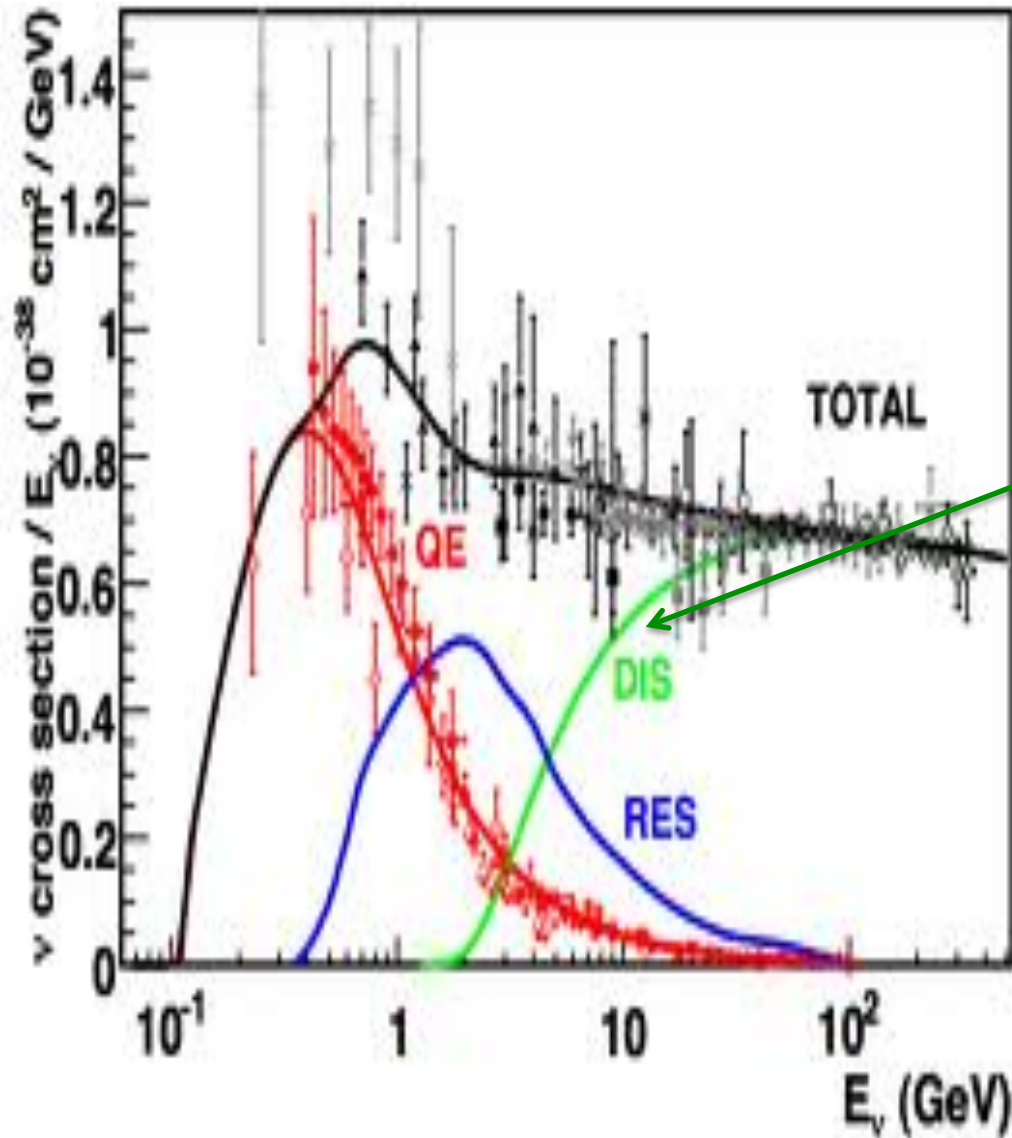
$x = Q^2 / 2M\nu$ = fraction of momentum carried by quark)

$x=1$ for quasielastic scattering)

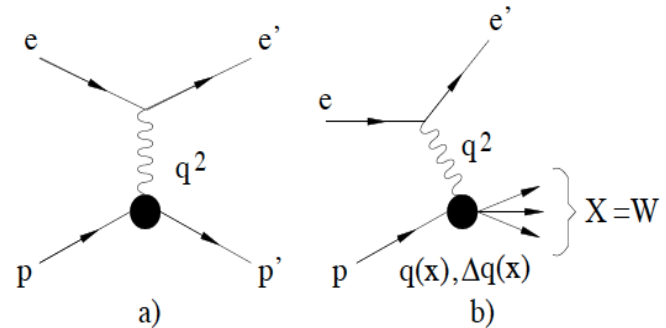
Philosophy

1. *Electron Scattering data needs to be parametrized in a simple way, and then used to predict the vector part of the interaction.* We need to predict vector parts of both the longitudinal and transverse structure functions (response functions, form factors) at the level of a few percent, using electron scattering measurements for the appropriate reactions. *All modeling parameters should be extracted from data.*
2. *If all processes are parametrized in terms of vector and axial structure functions (forms factors/response functions), then by construction they describes all kinematic distributions of the final state lepton, and are applicable at all energies for electron scattering as well as neutrinos and antineutrinos.*
3. *Neutrino scattering data can then be used to constrain the axial structure functions (response functions, form factors)*
4. *We also need the nuclear corrections to the vector and axial structure functions.*

In the 1-10 GeV region all three processes (QE, Resonance, Inelastic Continuum (called "DIS" in the figure below) contribute to neutrino charged current total cross section



A. Bodek



The name DIS here is used loosely for inelastic processes with $W > 1.8$ GeV (in the continuum at all Q^2 , including $Q^2 = 0$).

(nominat definition of DIS requires $Q^2 > 1$ GeV²).

Inelastic includes resonances and continuum, i.e. everything that is not QE.

Longitudinal vs Transverse (Scattering from Quarks, structure function description)

- Transverse means polarization of the electric field perpendicular to the direction of motion. i.e. the spin/helicity is along the the direction of motion (e.g. real photons).
- Since quarks are very low mass, they have +-helicity. Therefore, the absorption of transverse photons results in spin/helicity flip of the quarks (which is the dominant process at large Q^2).
- Longitudinal means that electric field is parallel the direction of motion. This is only possible for off-shell virtual photons. This means that the photons can only be absorbed by quarks which have a transverse momentum (e.g. from gluon emission, or binding the nucleon, target mass).
- For charged current scattering from individual quarks: vector=axial

2 Electron-nucleon and muon-nucleon scattering

terms of the structure functions $\mathcal{F}_1 = MW_1(x, Q^2)$, $\mathcal{F}_2 = \nu W_2(x, Q^2)$ and $\mathcal{F}_3 = \nu W_3(x, Q^2)$:

Structure function description

$$\frac{d^2\sigma}{d\Omega dE'}(E_0, E', \theta) = \frac{4\alpha^2 E'^2}{Q^4} \cos^2(\theta/2) \times [\mathcal{F}_2(x, Q^2)/\nu + 2 \tan^2(\theta/2) \mathcal{F}_1(x, Q^2)/M]$$

$$\frac{d^2\sigma}{d\Omega dE'} = \Gamma [\sigma_T(x, Q^2) + \epsilon \sigma_L(x, Q^2)]$$

Transverse and longitudinal description

$$\Gamma = \frac{\alpha K E'}{4\pi^2 Q^2 E_0} \left(\frac{2}{1 - \epsilon} \right)$$

$$\epsilon = \left[1 + 2 \left(1 + \frac{Q^2}{4M^2 x^2} \right) \tan^2 \frac{\theta}{2} \right]^{-1}$$

$$K = \frac{Q^2(1-x)}{2Mx}$$

Virtual boson polarization is a function of y (or angle)

Ratio of L/T

$$\mathcal{R}(x, Q^2) = \frac{\sigma_L}{\sigma_T} = \frac{\mathcal{F}_2}{2x\mathcal{F}_1} \left(1 + \frac{4M^2 x^2}{Q^2} \right) - 1 = \frac{\mathcal{F}_L}{2x\mathcal{F}_1}$$

Relation between the two descriptions.

$$\mathcal{F}_1 = \frac{MK}{4\pi^2 \alpha} \sigma_T, \quad \text{Purely transverse}$$

$$\mathcal{F}_2 = \frac{\nu K (\sigma_L + \sigma_T)}{4\pi^2 \alpha \left(1 + \frac{Q^2}{4M^2 x^2} \right)} \quad \text{Sum of T and L}$$

Since R is small at high Q^2 , we use mixed description in terms of $\mathcal{F}_2, R, \mathcal{F}_3$ (shown below for neutrino scattering)

$$\frac{d^2\sigma^{\nu(\bar{\nu})}}{dx dy} = \frac{G_F^2 M E_\nu}{\pi} \left(\left[1 - y \left(1 + \frac{Mx}{2E_\nu} \right) + \frac{y^2}{2} \left(\frac{1 + \left(\frac{2Mx}{Q} \right)^2}{1 + R} \right) \right] \mathcal{F}_2 \pm \left[y - \frac{y^2}{2} \right] x \mathcal{F}_3 \right)$$

For neutrinos, the structure functions have both vector and axial components)

Relations between electric and magnetic form factors and structure functions for elastic electron scattering on free nucleons

$$W_{1p}^{elastic} = \delta(\nu - \frac{Q^2}{2M}) \tau |G_{Mp}(Q^2)|^2$$

$$W_{1n}^{elastic} = \delta(\nu - \frac{Q^2}{2M}) \tau |G_{Mn}(Q^2)|^2$$

and

$$W_{2p}^{elastic} = \delta(\nu - \frac{Q^2}{2M}) \frac{[G_{Ep}(Q^2)]^2 + \tau [G_{Mp}(Q^2)]^2}{1 + \tau}$$

$$W_{2n}^{elastic} = \delta(\nu - \frac{Q^2}{2M}) \frac{[G_{En}(Q^2)]^2 + \tau [G_{Mn}(Q^2)]^2}{1 + \tau}$$

$$R_{p,n}^{elastic}(x = 1, Q^2) = \frac{\sigma_L^{elastic}}{\sigma_T^{elastic}} = \frac{4M^2}{Q^2} \left(\frac{G_E^2}{G_M^2} \right)$$

Here, $\tau = Q^2/4M_{p,n}^2$, where $M_{p,n}$ are the masses of proton and neutron. Therefore, G_{Mp} and G_{Mn} contribute to the transverse virtual photo-absorption cross section, and G_{Ep} and G_{En} contribute to the longitudinal cross section.

$$\mathcal{F}_A \approx -1.267 / (1 + Q^2/M_A^2)^2$$

For Neutrino QE scattering: Vector form factors are known from electron scattering. But we also have axial form factors

$$W_{1-Qelastic}^{v-vector} = \delta\left(\nu - \frac{Q^2}{2M}\right) \tau |G_M^V(Q^2)|^2,$$

$$W_{1-Qelastic}^{v-axial} = \delta\left(\nu - \frac{Q^2}{2M}\right) (1 + \tau) |\mathcal{F}_A(Q^2)|^2,$$

$$W_{2-Qelastic}^{v-vector} = \delta\left(\nu - \frac{Q^2}{2M}\right) |\mathcal{F}_V(Q^2)|^2,$$

$$W_{2-Qelastic}^{v-axial} = \delta\left(\nu - \frac{Q^2}{2M}\right) |\mathcal{F}_A(Q^2)|^2,$$

$$W_{3-Qelastic}^v = \delta\left(\nu - \frac{Q^2}{2M}\right) |2G_M^V(Q^2)\mathcal{F}_A(Q^2)|,$$

where

$$G_E^V(Q^2) = G_E^p(Q^2) - G_E^n(Q^2),$$

$$G_M^V(Q^2) = G_M^p(Q^2) - G_M^n(Q^2).$$

and

$$|\mathcal{F}_V(Q^2)|^2 = \frac{[G_E^V(Q^2)]^2 + \tau [G_M^V(Q^2)]^2}{1 + \tau}.$$

$$\sigma_T^{vector} \propto \tau |G_M^V(Q^2)|^2; \quad \sigma_T^{axial} \propto (1 + \tau) |\mathcal{F}_A(Q^2)|^2,$$

$$\sigma_L^{vector} \propto (G_E^V(Q^2))^2; \quad \sigma_L^{axial} = 0.$$

Jupiter Collaboration (Jlab E04-001)

A. Bodek, Cynthia Keppel, Eric Christy

Spokespersons

- We have measured electron scattering cross sections on nucleon and nuclear targets in the few GeV region in 2004 and 2007
- We use these new measurements in conjunction with all previous electron scattering data to extract the vector contributions (form factors, structure functions, QE nuclear response functions, etc.) to neutrino cross sections on protons, neutrons and nuclear targets in the few GeV region. (Note: these cross sections have not been used yet in fitting the Bodek-Yang model).
- Jupiter is Complementary to the MINERvA neutrino experiment

Issues in modeling for $Q^2 < 1 \text{ GeV}^2$

- First, need model all processes for vector structure functions for free neutrons and protons for all Q^2 and ν using electron scattering data and photoproduction data ($Q^2=0$) on hydrogen and deuterium.

THIS IS MUST BE DONE First

- For modeling neutrinos high Q^2 $V=A$. How much is V different from A at low Q^2 ($Q^2 < 1 \text{ GeV}^2$)
- By gauge invariance the vector structure function F_2 for all inelastic processes goes to zero at $Q^2=0$. This is not required for axial structure functions. This $Q^2=0$ constraint needs to be modeled.
- Need to model all nuclear modifications of the scattering when protons and neutrons are bound in a nucleus
- How are those nuclear modifications different for vector and axial structure functions.

Is it possible to model inelastic scattering at low Q^2

Well, use parton distribution functions. PDFs are well known, and from these you can calculate both electron and neutrino scattering using the quark couplings. PDFs have been fit to high Q^2 data and with QCD evolution they work down $Q^2 = 0.8 \text{ GeV}^2$

However, QCD evolution is not enough. QCD breaks down at low Q^2 and higher twist effects become large. All QCD sum rules break down.

One example, Energy momentum Sum Rule (total momentum taking up by quarks and gluons)=1 has large QCD corrections.

Another example, the Gross-Llewellyn Smith sum rule (total number of valence quarks in the nucleon is 3) has large QCD and higher twist corrections.

$$\int_0^1 \frac{x F_3(x)}{x} dx = 2.13 \pm 0.38 (\text{stat}) \pm 0.26 (\text{syst}). \quad \overline{Q^2} \sim 1.7 \text{ GeV}^2.$$

$$GLS(Q^2) = 3 \left[1 - \alpha_s(Q^2)/\pi + O(\alpha_s^2) - \frac{8}{27} \frac{\langle\langle O \rangle\rangle}{Q^2} \right] \quad \alpha_s(Q^2) = b_0 / \ln(Q^2/\Lambda^2)$$

So GLS sum rules blows up as we go to very low Q^2

Sum rules continued

$$GLS(Q^2) = 3 \left[1 - \alpha_s(Q^2)/\pi + O(\alpha_s^2) - \frac{8}{27} \frac{\langle\langle O \rangle\rangle}{Q^2} \right] \quad \alpha_s(Q^2) = b_0 / \ln(Q^2/\Lambda^2)$$

LO Parton Distribution Functions are fit to high Q^2 data assuming QCD evolution.

LO PDF fits neglect the higher order QCD and low Q^2 twist corrections (which are large). In LO the fits assume that GLS sum rule = 3. i.e. All of the higher order QCD corrections are ignored

Can we use QCD NLO or NNLO PDFs. *After all We are scattering from quarks at all Q^2*

Well: NLO or NNLO do not work. Both NLO and NNLO corrections blow up at low Q^2 . Higher twist corrections also blow up. So the only thing we can use at low Q^2 are LO PDFs

So how do we model

inelastic scattering at low Q^2 at the level of a few percent using PDFs if there are so many corrections?

→ We can do it if we get all the corrections from the data.

Require known constraints to get forms of the corrections

By gauge invariance the vector structure function F_2 for all inelastic processes goes to zero at $Q^2=0$. So the structure functions cannot blow up at low Q^2 .

Possible solution 1: Freeze the PDFs at $Q^2=0.8 \text{ GeV}^2$. Then multiply them by a low Q^2 K factor: for example $K = Q^2/(Q^2+C)$.

Use low Q^2 electron scattering data to fit for C. Then the F_2 structure function will go to zero at $Q^2=0$ by construction. When we do that, we find that $C=0.18 \text{ GeV}^2$.

But is this the right functional form? Is it the same for u and d quarks. Is it the same for valence and sea quarks. Is it independent of x. Is there any theoretical motivation for this form?

One Check on C: Use photo-production data

On hydrogen and deuterium

This is great for the vector structure functions

What about the axial structure function.

We also need constraints that apply to the axial structure functions.

$$\begin{aligned}\sigma(\gamma p) &= \frac{4\pi^2\alpha}{Q^2} \mathcal{F}_2^{e/\mu}(x, Q^2) \\ &= \frac{0.112 \text{ mb}}{Q^2} \mathcal{F}_2^{e/\mu}(x, Q^2)\end{aligned}$$

Additional constraints

At $Q^2=0$, $x = 0$. \rightarrow So this is a problem in using PDFs at $Q^2=0$.

We need PDFs which are a function Q^2 and v .

And PDFs are functions of x and Q^2 .

Possible Solution 2 use a scaling variable that does not go to zero at $Q^2=0$.

replace x with: $X_w = (Q^2 + B) / 2M v$.

We can use data to fit for the parameter B .

But is this enough? Is there any theoretical motivation for this form?

Also, How do we account for higher order QCD corrections, target mass effects, higher twist effects which are important at large x .

Impose more constraints: The Adler Sum rule

The Adler sum rule in QCD is just the statement that the number of u quarks (which is 2) minus the number of d quarks (which is 1) equals 1. We can measure this number using neutrino, neutrino vector or neutrino axial structure functions:

$$\int_{\nu_0}^{\infty} W_{2n-sc}^{\nu-vector}(\nu, Q^2) d\nu - \int_{\nu_0}^{\infty} W_{2p-sc}^{\nu-vector}(\nu, Q^2) d\nu = 1$$

$$\int_{\nu_0}^{\infty} W_{2n-sc}^{\nu-axial}(\nu, Q^2) d\nu - \int_{\nu_0}^{\infty} W_{2p-sc}^{\nu-axial}(\nu, Q^2) d\nu = 1$$

Or equivalently, the Adler sum rule can be written as the difference between the antineutrino and neutrino structure functions on protons (either axial or vector)

$$\int_0^1 (dx/x) [F_2^{\bar{\nu}}(x) - F_2^{\nu}(x)] = 1$$

$$U - D = 1$$

The Adler sum rule is a current algebra sum rule, so unlike QCD sum rules it is exact and it is valid at ALL Q^2 , including $Q^2=0$. So it has a lot to tell us about the form of the structure functions at low Q^2 .

If we separate the quasielastic part and the inelastic part of the Adler Sum rules and get.

$$\int_{\nu_0}^{\infty} W_{2n-sc}^{\nu-vector}(\nu, Q^2) d\nu - \int_{\nu_0}^{\infty} W_{2p-sc}^{\nu-vector}(\nu, Q^2) d\nu = 1 - |F_V(Q^2)|^2$$

$$|F_V(Q^2)|^2 = \frac{[G_E^V(Q^2)]^2 + \tau [G_M^V(Q^2)]^2}{1 + \tau}$$

$$\int_{\nu_0}^{\infty} W_{2n-sc}^{\nu-axial}(\nu, Q^2) d\nu - \int_{\nu_0}^{\infty} W_{2p-sc}^{\nu-axial}(\nu, Q^2) d\nu = 1 - |\mathcal{F}_A(Q^2)|^2$$

$$\mathcal{F}_A \approx -1.267 / (1 + Q^2/M_A^2)^2$$

At high Q^2 both F_V and \mathcal{F}_A are zero and the sum rule is just $U-D = 1$

Now: If we multiply the inelastic vector u and d LO PDFs by $1 - |F_V(Q^2)|^2$

And multiply the inelastic axial u and d LO PDFS by $1 - |\mathcal{F}_A(Q^2)|^2$

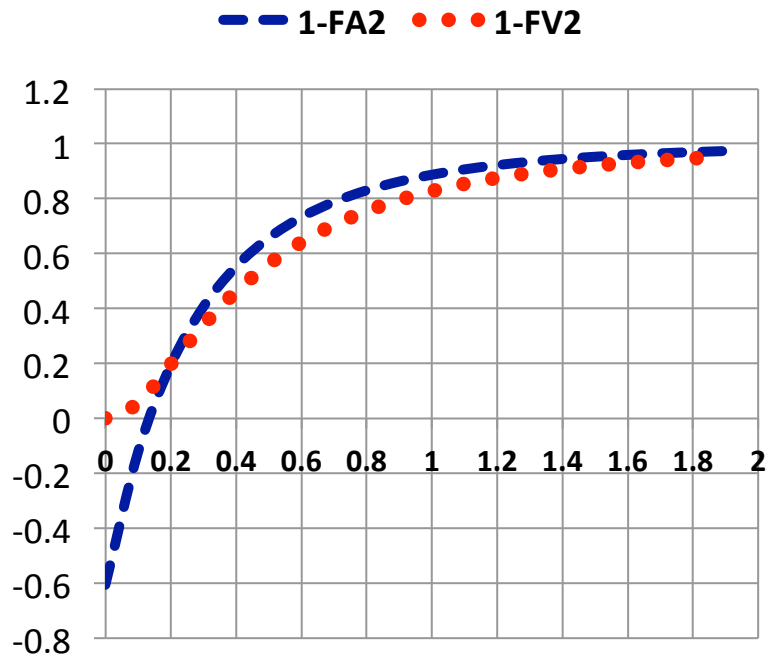
Then is Adler sum rule satisfied at all Q^2 ??

Multiply the inelastic vector u and d LO PDFs by

$$: 1 - |F_V(Q^2)|^2$$

Multiply the inelastic axial u and d LO PDFS by

$$: 1 - |F_A(Q^2)|^2$$



This figure indicates that it looks like the axial and vector PDFs are the same down to $Q^2 = 0.2 \text{ GeV}^2$. Everything works except for the axial part below $Q^2 = 0.2 \text{ GeV}^2$.

For $Q^2 < 0.2 \text{ GeV}^2$ we find that if we add the contribution of the Δ resonance it cancels the -0.6 at $Q^2 = 0$, and the axial Adler sum rule is satisfied..

This illustrates how the vector inelastic PDFs goes to zero at $Q^2 = 0$. We also see that the axial inelastic PDFs are also very small near $Q^2 = 0$.

Note: the Adler sum rule is just the difference between U_{valence} and D_{valence} . The K factor can be different for U and D, as long as the Adler sum rule is satisfied.

History of Inelastic Sum rules C. H. Llewellyn Smith hep-ph/981230

Talk given at the Sid Drell Symposium

SLAC, Stanford, California, July 31st, 1998

Gottfried noted that in the 'breathhtakingly crude' naive three-quark model the second term in the following equation vanishes for the proton (it also vanishes for the neutron, but neutrons are not mentioned):

$$\sum_{i,j} Q_i Q_j \equiv \sum_i Q_i^2 + \sum_{i \neq j} Q_i Q_j. \quad (5)$$

Thus for any charge-weighted, flavour-independent, one-body operator all correlations vanish, and therefore using the closure approximation the following sum rule can be derived:

$$\int_{\nu_0} W_2^{ep}(\nu, q^2) d\nu = 1 - \frac{G_E^2 - q^2 G_M^2 / 4m^2}{1 - q^2 / 4m^2}, \quad (6)$$

where ν_0 is the inelastic threshold (the methods used to derive this sum rule are those that have long been used to derive sum rules in atomic and nuclear physics, for example

The above equation uses Closure (Identity operator = 1 in QM i.e. sum over all states.) But it is only valid for 3 quarks in the proton (i.e. valence quarks). If you include the sea quarks, you get infinity, unless you subtract neutron and proton structure functions (which then yields the Gottfried Sum rule)^{A. Bodek}

For reference, when we include sea quarks then the Gottfried Sum rule at high Q² takes the following form.

$$\int \left(F_2^{ep}(x, q^2) - F_2^{en}(x, q^2) \right) \frac{dx}{x} = \frac{1}{3}(n_u + n_{\bar{u}} - n_d - n_{\bar{d}}) = \frac{1}{3} + \frac{2}{3}(n_{\bar{u}} - n_{\bar{d}}),$$

Now closure, Gottfried suggests somewhat different low Q² K factor for valence quarks.

$$\int_{\nu_0} W_2^{ep}(\nu, q^2) d\nu = 1 - \frac{G_E^2 - q^2 G_M^2 / 4m^2}{1 - q^2 / 4m^2}$$

Where the right hand side is just W_{2e-p} (elastic)

$$W_2^{el}(q^2) = \frac{G_E^2(q^2) + \tau G_M^2(q^2)}{1 + \tau}, \quad \tau = \frac{q^2}{4M^2}$$

Note: at low Q²

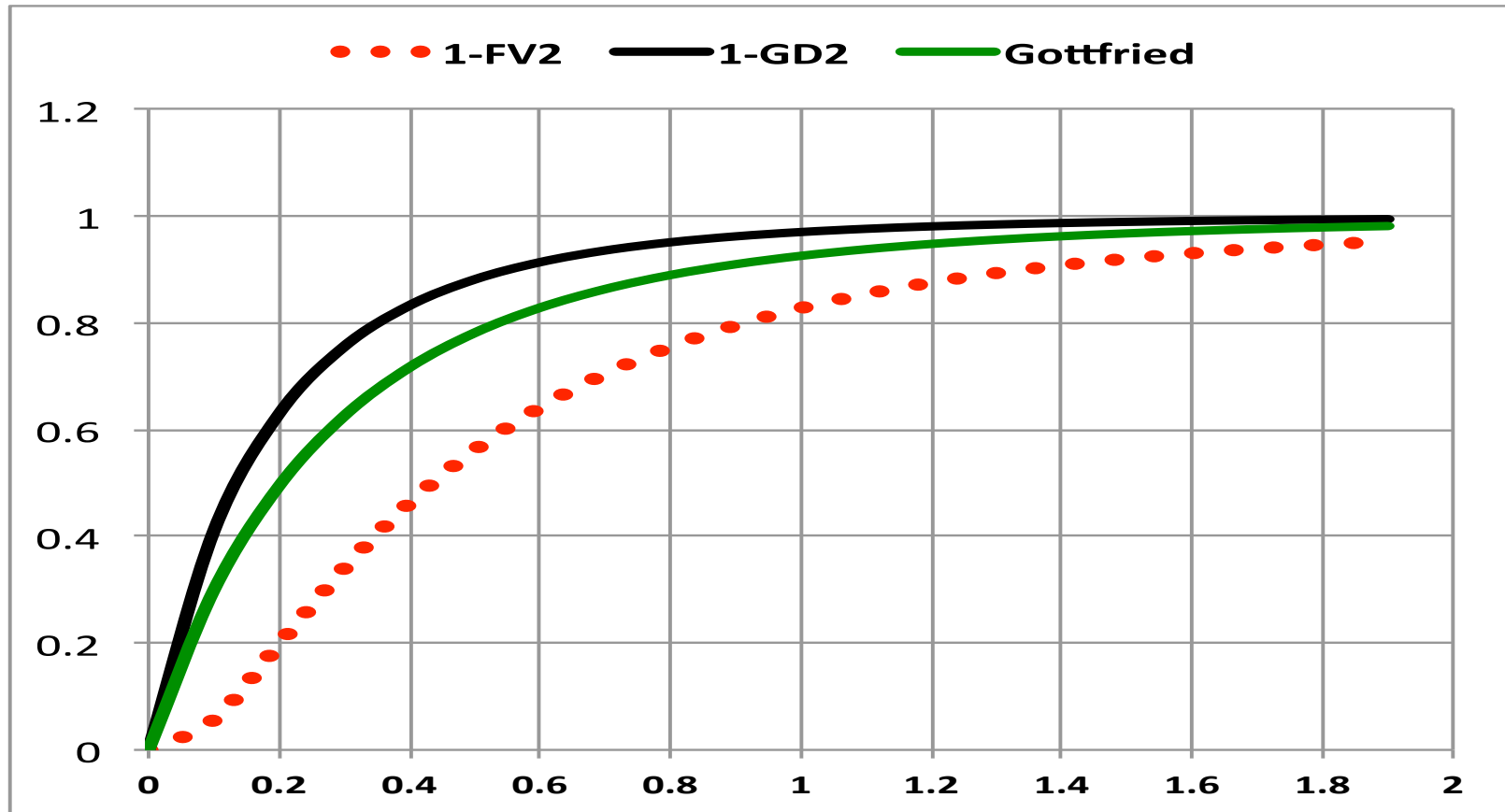
$$\begin{aligned} [1 - W_2^{el}] &= 1 - 1 / (1 + Q^2 / 0.71)^4 \\ &= 1 - (1 - 4Q^2 / 0.71) = \\ &= 1 - (1 - Q^2 / 0.178) = \\ &\rightarrow Q^2 / 0.178 \text{ as } Q^2 \rightarrow 0 \end{aligned}$$

Versus Our GRV98 fit with

$$Q^2 / (Q^2 + C) \rightarrow Q^2 / C$$

$$c = 0.1797 \pm 0.0036$$

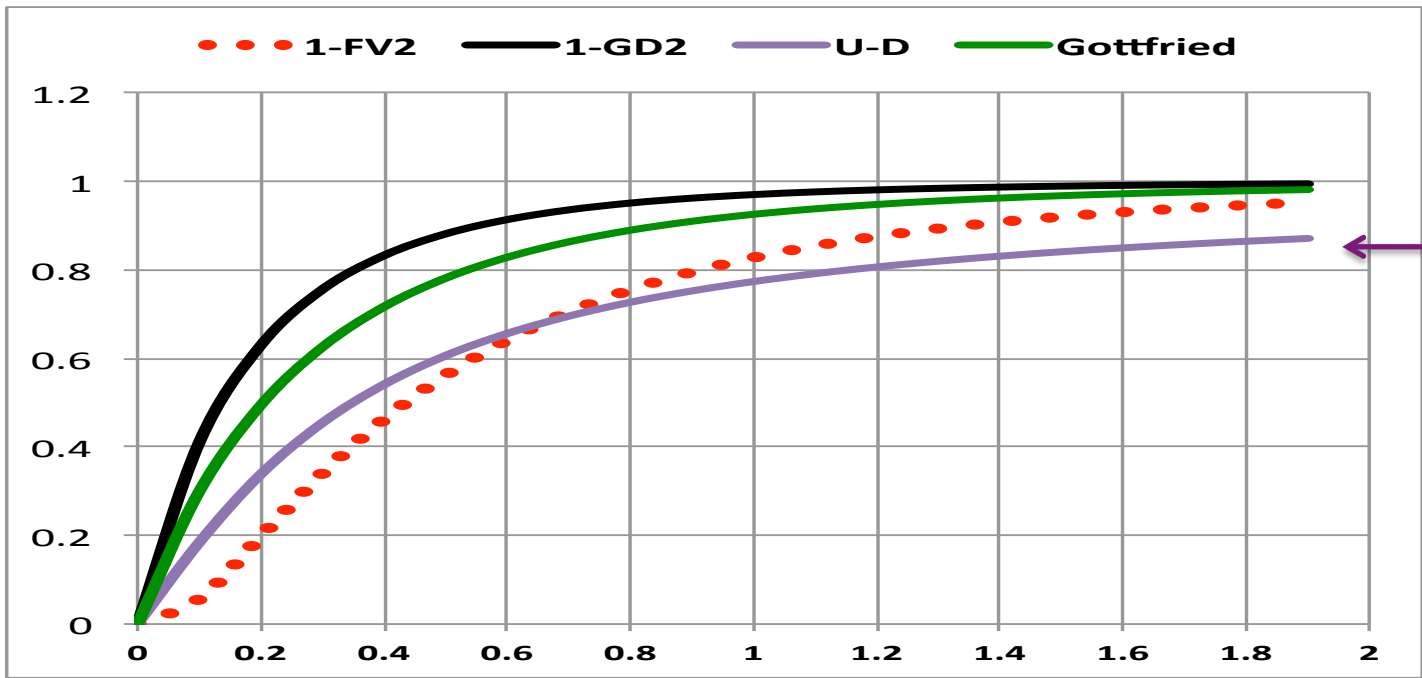
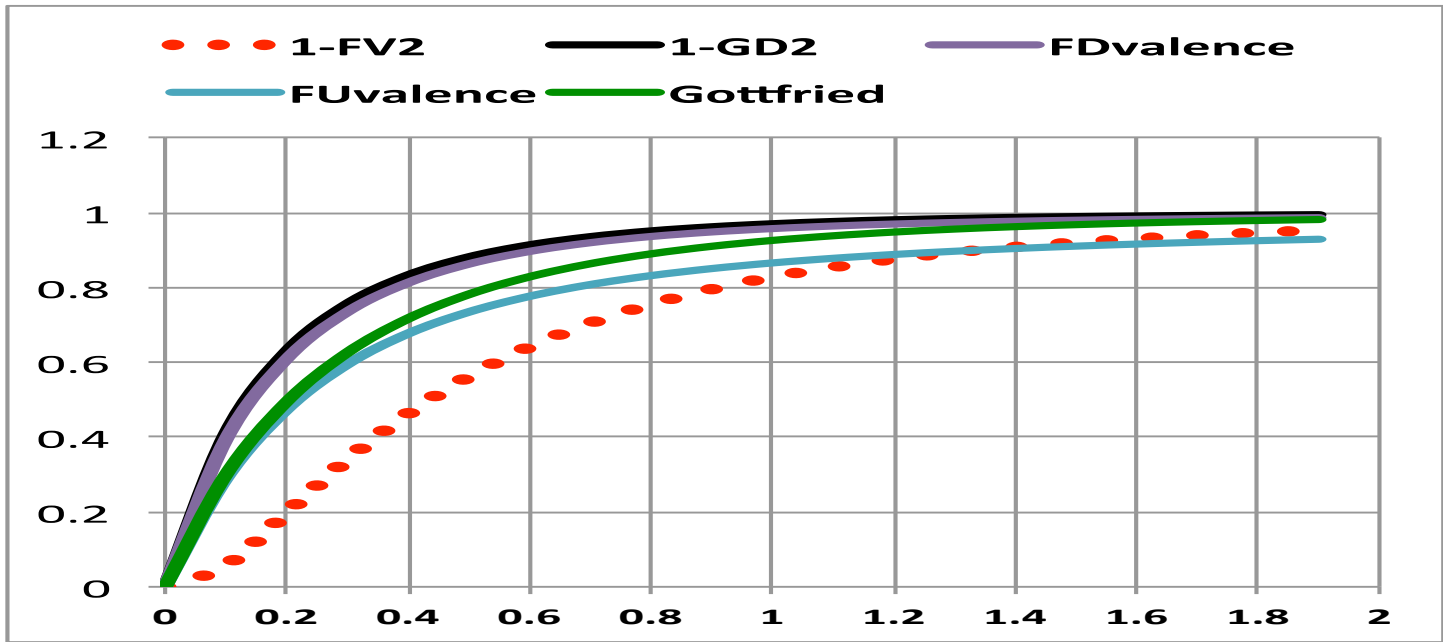
So now we know where C=0.18 comes from



Therefore, we allow the K factors for U and D valence quarks to be different in our fits, Include both electroproduction on H and D and photoproduction data for H And D.

H and D information allows us to Get the K factor for Uv and Dv separately.

$$\begin{aligned}
 K_{valence-up}^{vector}(Q^2) &= K^{LW} [1 - G_D^2(Q^2)] \\
 &\quad \times \left(\frac{Q^2 + C_{v2u}}{Q^2 + C_{v1u}} \right) \\
 K_{valence-down}^{vector}(Q^2) &= K^{LW} ([1 - G_D^2(Q^2)] \\
 &\quad \times \left(\frac{Q^2 + C_{v2d}}{Q^2 + C_{v1d}} \right)
 \end{aligned} \tag{21}$$



Effective Leading Order PDFs (Bodek-Yang Scaling Variable)

- The GRV98 PDFs are leading order. They start at a $Q^2=0.8 \text{ GeV}^2$, and are evolved to higher Q^2 . The parameters of the PDFs are extracted from high Q^2 data. They are a function of x and Q^2 .
- However, when a quark of mass M_i is bound in the proton of mass M , we can derive using energy conservation that the correct scaling variable (i.e. the fractional momentum carried by the quarks) is given by

$$\xi = \frac{2xQ'^2}{Q^2(1 + \sqrt{1 + 4M^2x^2/Q^2})}, \quad (11)$$

where

$$2Q'^2 = [Q^2 + M_f^2 - M_i^2] + \sqrt{(Q^2 + M_f^2 - M_i^2)^2 + 4Q^2(M_i^2 + P_T^2)}$$

For cases such as charm production the mass of the final state quark is M_f

When mass of the initial and final state quarks is zero, and the P_T of the initial quark is zero, Equation 11 yields the familiar target mass scaling variable (sometimes known as the Nachtmann variable, or the Georgi-Politzer target mass variable) that accounts for quark binding in the proton

$$\xi_{TM} = \frac{Q^2}{M\nu[1 + \sqrt{1 + Q^2/\nu^2}]},$$

$$\xi = \frac{2xQ'^2}{Q^2(1 + \sqrt{1 + 4M^2x^2/Q^2})}, \quad (11)$$

where

$$2Q'^2 = [Q^2 + M_f^2 - M_i^2] + \sqrt{(Q^2 + M_f^2 - M_i^2)^2 + 4Q^2(M_i^2 + P_T^2)}$$

The Bodek-Yang scaling variable adds parameter B to the numerator to take into account the initial state quark PT and an effective final state quark mass from multi gluon emission. The parameter B also allows us to use PDFs in the photoproduction limit (Q²=0).

We also add a parameter A to the denominator to enhance the target mass effects to account for higher order QCD and higher twist corrections. **The full scaling variable is:**

$$\xi_w = \frac{2x(Q^2 + M_f^2 + B)}{Q^2[1 + \sqrt{1 + 4M^2x^2/Q^2}] + 2Ax}, \quad (12)$$

or alternatively

$$\xi_w = \frac{(Q^2 + M_f^2 + B)}{M\nu[1 + \sqrt{1 + Q^2/\nu^2}] + A},$$

The parameters A and B are extracted from fits to the data. At Q²=0, the above scaling variable is not zero, so now the PDFs are functions of both **Q² and v**. At high Q² the scaling parameter is just $x = \mathbf{Q^2/2Mv}$, which is what variable that is used for the PDF fits at high Q².

Effective LO PDFs at low Q^2

Only Leading Order PDFs can be used. NLO and NNLO PDFs and sum rules blow up at low Q^2 ($<0.8 \text{ GeV}^2$). So we use GRV98 LO PDFS

All low Q^2 corrections are now modeled simply using the following two modifications.

(a) Using a new scaling variable ξ_w that reflects the fractional momentum carried by the quarks at low Q^2 and also accounts for the additional corrections.

(b) Using multiplicative K factors, $K(Q^2)$ to account for higher order corrections, and non-perturbative higher twist effects as we approach $Q^2 = 0$. The factors satisfy the constraints from the Adler Sum rule, Gottfried Closure Sum rule, and yield the correct photoproduction cross section.

Original Bodek – Yang Model (currently implemented in neutrino MC's)

Include low Q K factors

1. The GRV98 [24] LO Parton Distribution Functions (PDFs) are used to describe $\mathcal{F}_{2,LO}^{e/\mu}(x, Q^2)$. The minimum Q^2 value for these PDFs is 0.8 (GeV/c)^2 .
2. The scaling variable x is replaced with the scaling variable ξ_w as defined in Eq. 12. Here,

Use New scaling variable

$$\xi_w = \frac{(Q^2 + M_f^2 + B)}{M\nu[1 + \sqrt{1 + Q^2/\nu^2}] + A},$$

We freeze the evolution of the GRV98 PDFs at a value of $Q^2 = 0.80 \text{ (GeV/c)}^2$. Below this Q^2 , \mathcal{F}_2 is given by;

$$\begin{aligned} \mathcal{F}_2^{e/\mu}(x, Q^2 < 0.8) = & \\ K_{valence}^{vector}(Q^2) \mathcal{F}_{2,LO}^{valence}(\xi_w, Q^2 = 0.8) & \\ + K_{sea}^{vector}(Q^2) \mathcal{F}_{2,LO}^{sea}(\xi_w, Q^2 = 0.8) & \end{aligned} \quad (19)$$

$$\begin{aligned} K_{sea}^{vector}(Q^2) &= \frac{Q^2}{Q^2 + C_s} \\ K_{valence}^{vector}(Q^2) &= [1 - G_D^2(Q^2)] \\ &\quad \times \left(\frac{Q^2 + C_{v2}}{Q^2 + C_{v1}} \right) \end{aligned} \quad (17)$$

Check that the PDFs also describe photoproduction data. Although F_2 goes to zero, the slope of F_2 vs Q^2 is directly related to the photoproduction cross section

$$\begin{aligned} \sigma(\gamma p) &= \frac{4\pi^2\alpha}{Q^2} \mathcal{F}_2^{e/\mu}(x, Q^2) \\ &= \frac{0.112 \text{ mb}}{Q^2} \mathcal{F}_2^{e/\mu}(x, Q^2) \end{aligned} \quad (18)$$

Original Bodek – Yang Model (currently implemented in neutrino MC's)

5. Finally, we fit for the parameters of the modified effective GRV98 LO PDFs (e.g. ξ_w) to inelastic charged lepton scattering data on hydrogen and deuterium targets (SLAC[20]/BCDMS[21]/NMC[22]/H1[32]). In this first iteration, only data with an invariant final state mass $W > 2 \text{ GeV}/c^2$ are included, where $W^2 = M^2 + 2M\nu - Q^2$.

GRV 98 PDFs with 5- parameters describe all electron, muon, HERA, photoproduction inelastic data on H and D for $W > 2 \text{ GeV}$. (From $Q^2=0$, to $Q^2=10,000 \text{ GeV}^2$). For neutrino data prediction, change quark electric charges to quark vector and axial coupling.

$$\mathcal{F}_2^{e/\mu}(x, Q^2) = \frac{Q^2}{Q^2 + \underline{0.380}} \mathcal{F}_{2,LO}^{sea}(\xi_w, Q^2) + (1 - G_D^2) \frac{Q^2 + \underline{0.431}}{Q^2 + \underline{0.544}} \mathcal{F}_{2,LO}^{valence}(\xi_w, Q^2),$$

where $\xi_w = \frac{2x(Q^2 + \underline{0.223})}{Q^2[1 + \sqrt{1 + (2Mx)^2/Q^2}] + \underline{2*0.419}x}$.

A	B	C_{v1}	C_{v2}	χ^2/ndf
<u>0.419</u>	<u>0.223</u>	<u>0.554</u>	<u>0.431</u>	1235/1200
C_{sea}			N	$\mathcal{F}_{valence}$
<u>0.380</u>			1.011	$[1 - G_D^2(Q^2)]$

Updated Bodek – Yang Model

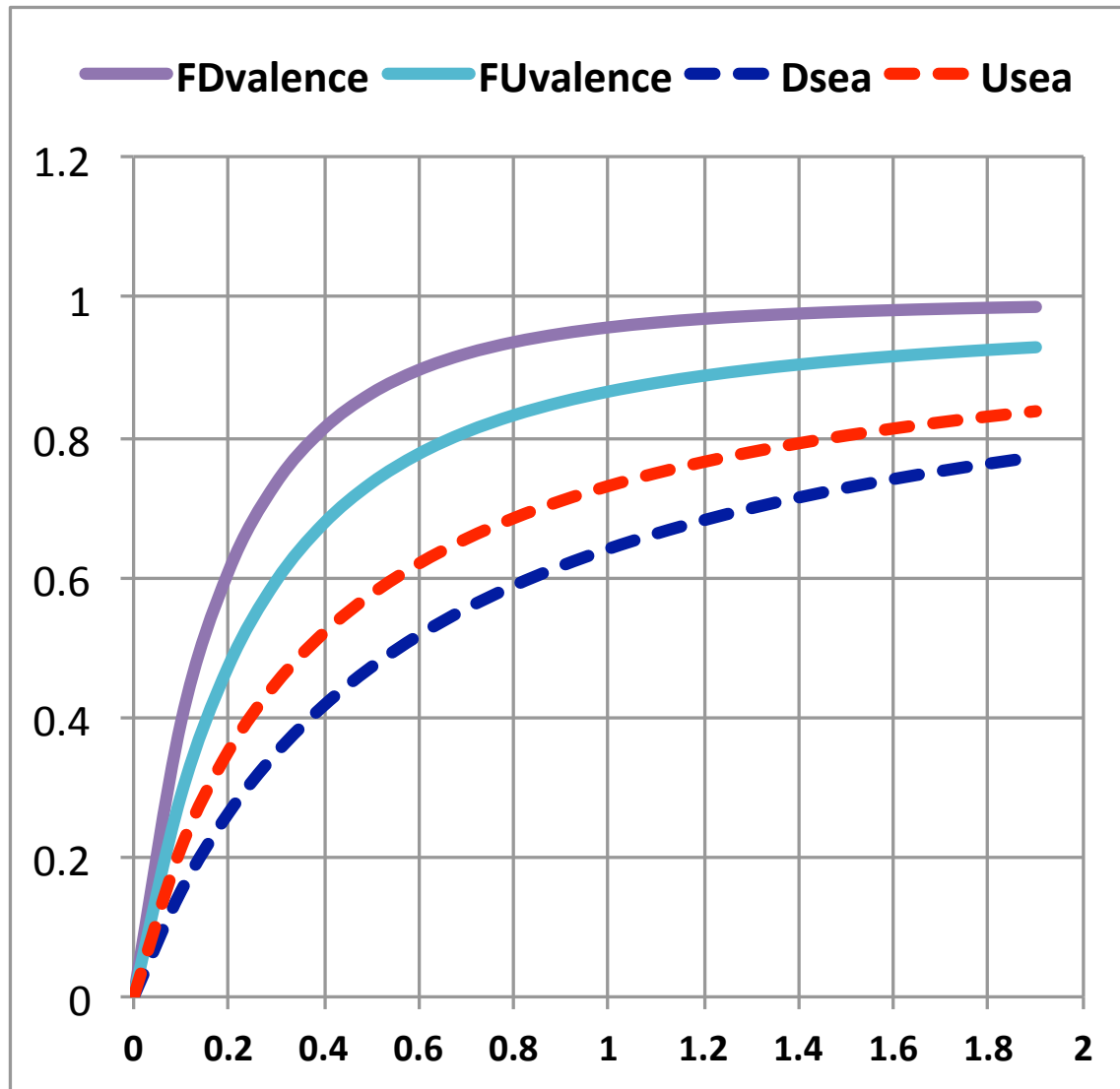
We have updated our model to have different low Q^2 K factors for up and down quarks, and include the photoproduction and data in the resonance region in the fit.

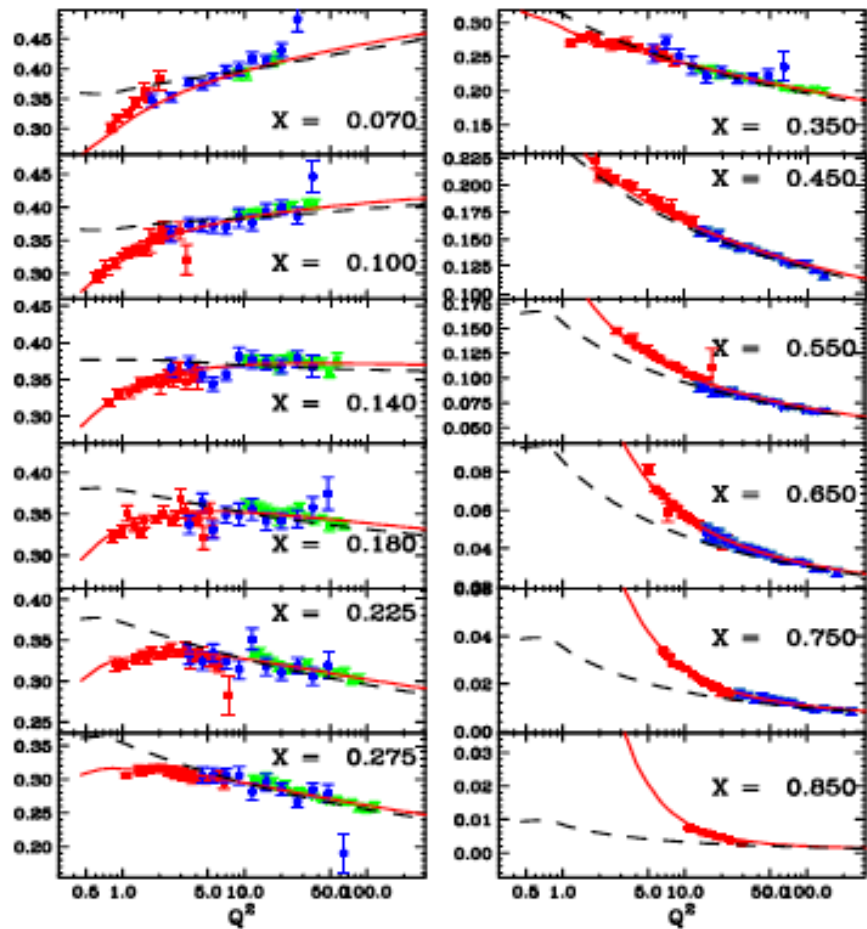
9 parameters describe all electron, muon, HERA, photoproduction data, And also Jlab data in the resonance region on H and D for $W > 1.6$ from $Q^2 = 0$ to $Q^2 = 10,000 \text{ GeV}^2$

$$\begin{aligned}
 K^{LW} &= \frac{\nu^2 + C^{low-\nu}}{\nu^2} \quad (W > 1.4 \text{ GeV}/c^2) \\
 K_{sea-strange}^{vector}(Q^2) &= \frac{Q^2}{Q^2 + C_{sea-strange}} \\
 K_{sea-up}^{vector}(Q^2) &= \frac{Q^2}{Q^2 + C_{sea}^{up}} \\
 K_{sea-down}^{vector}(Q^2) &= \frac{Q^2}{Q^2 + C_{sea}^{down}} \\
 K_{valence-up}^{vector}(Q^2) &= K^{LW} [1 - G_D^2(Q^2)] \\
 &\quad \times \left(\frac{Q^2 + C_{v2u}}{Q^2 + C_{v1u}} \right) \\
 K_{valence-down}^{vector}(Q^2) &= K^{LW} ([1 - G_D^2(Q^2)] \\
 &\quad \times \left(\frac{Q^2 + C_{v2d}}{Q^2 + C_{v1d}} \right)
 \end{aligned} \tag{21}$$

$$\xi_w = \frac{2x(Q^2 + M_f^2 + B)}{Q^2[1 + \sqrt{1 + 4M^2x^2/Q^2}] + 2Ax},$$

A	B	C_{v2d}	C_{v2u}
0.621	0.380	0.323	0.264
C_{sea}^{down}	C_{sea}^{up}	C_{v1d}	C_{v1u}
0.561	0.369	0.341	0.417
$C_{sea}^{strange}$	$C^{low-\nu}$	$F_{valence}$	N
0.561	0.218	$[1 - G_D^2(Q^2)]$	1.026





Fixed target electron and muon data on H (left) and D (right).

Dashed is GRV98. Red is GRV98 + Bodek Yang

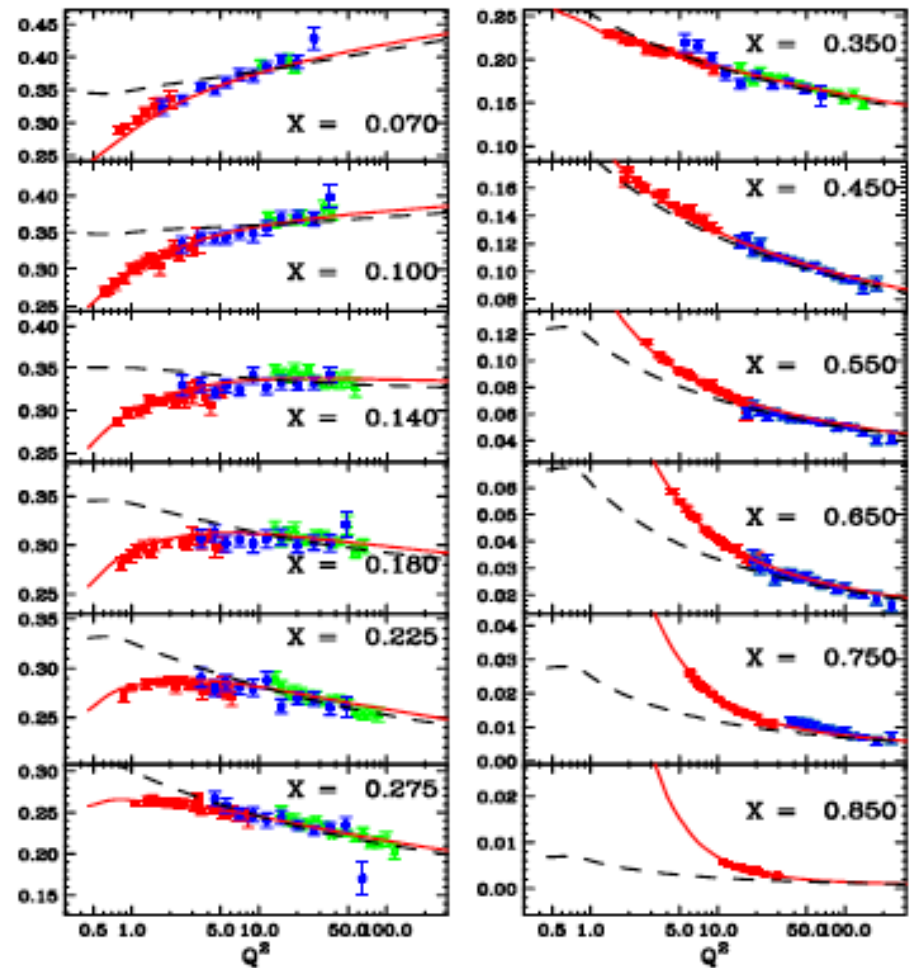


Fig. 2. The effective LO PDF model compared to charged lepton \mathcal{F}_2 experimental data (SLAC, BCDMS, NMC) at high x (these data are included in our fit) :[top] \mathcal{F}_2 proton, [bot] \mathcal{F}_2 deuteron. The solid lines are our fit, and the dashed lines are GRV98 .

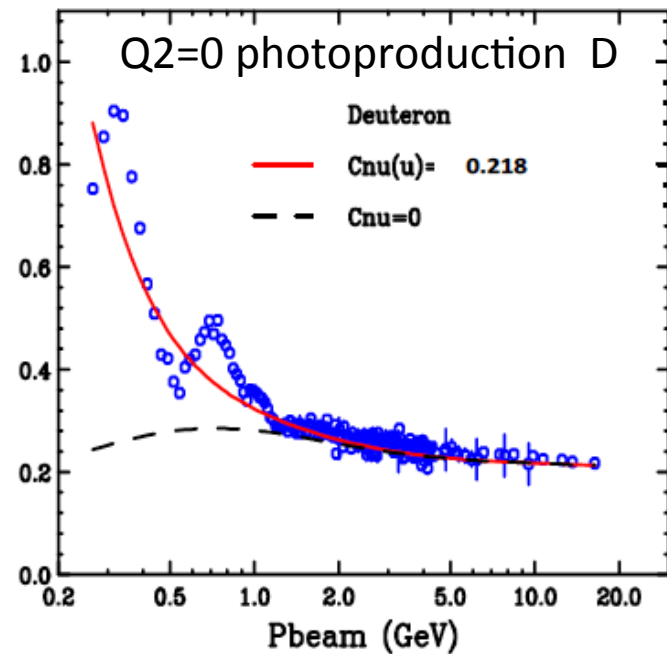
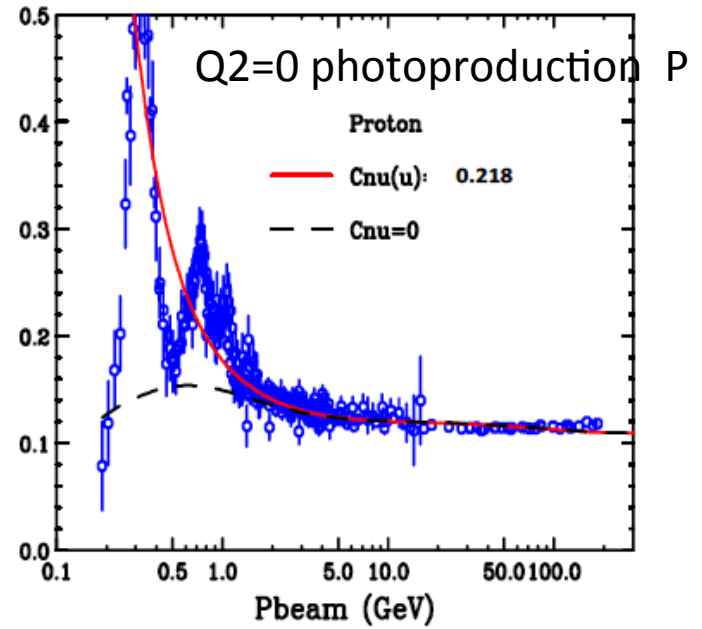
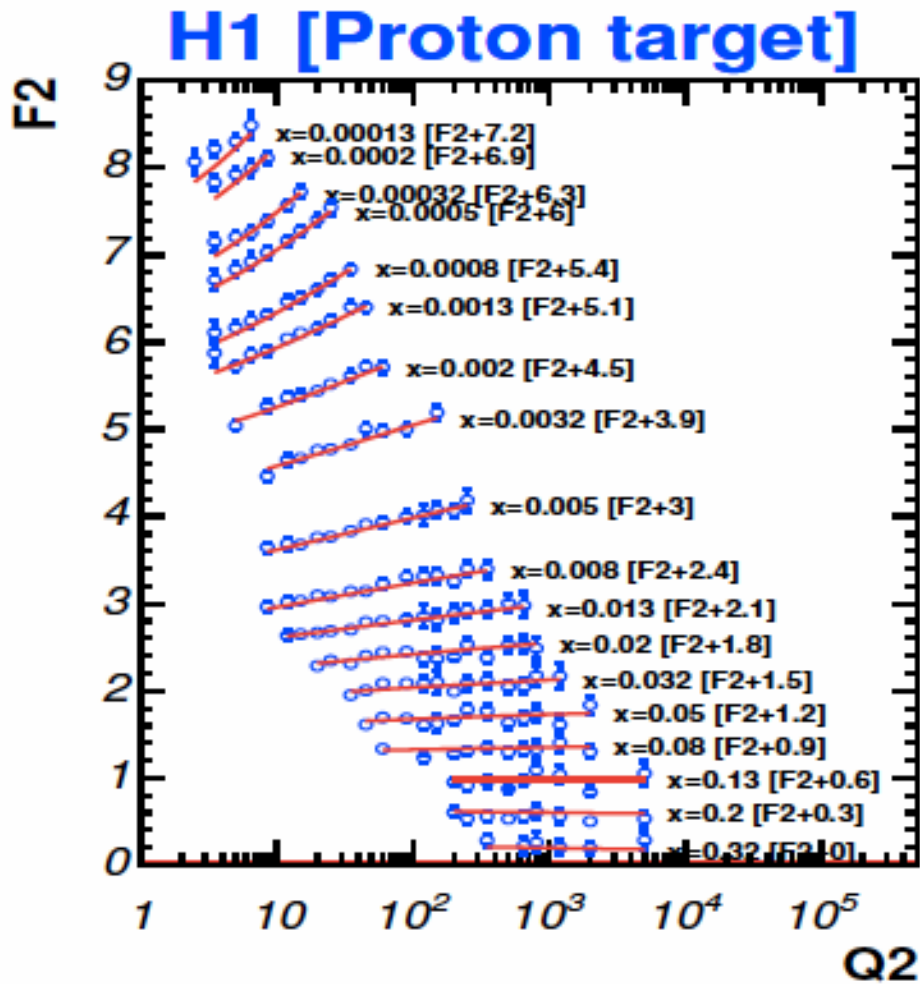


Fig. 3. The effective LO PDF model compared to charged lepton \mathcal{F}_2 experimental data at low x from H1 (these data are included in our fit).

Extreme range of Q^2 0 to 10,000 GeV^2 Works for $W > 1.5$ GeV (above the Δ resonance)

Resonance Region and Quark Hadron Duality

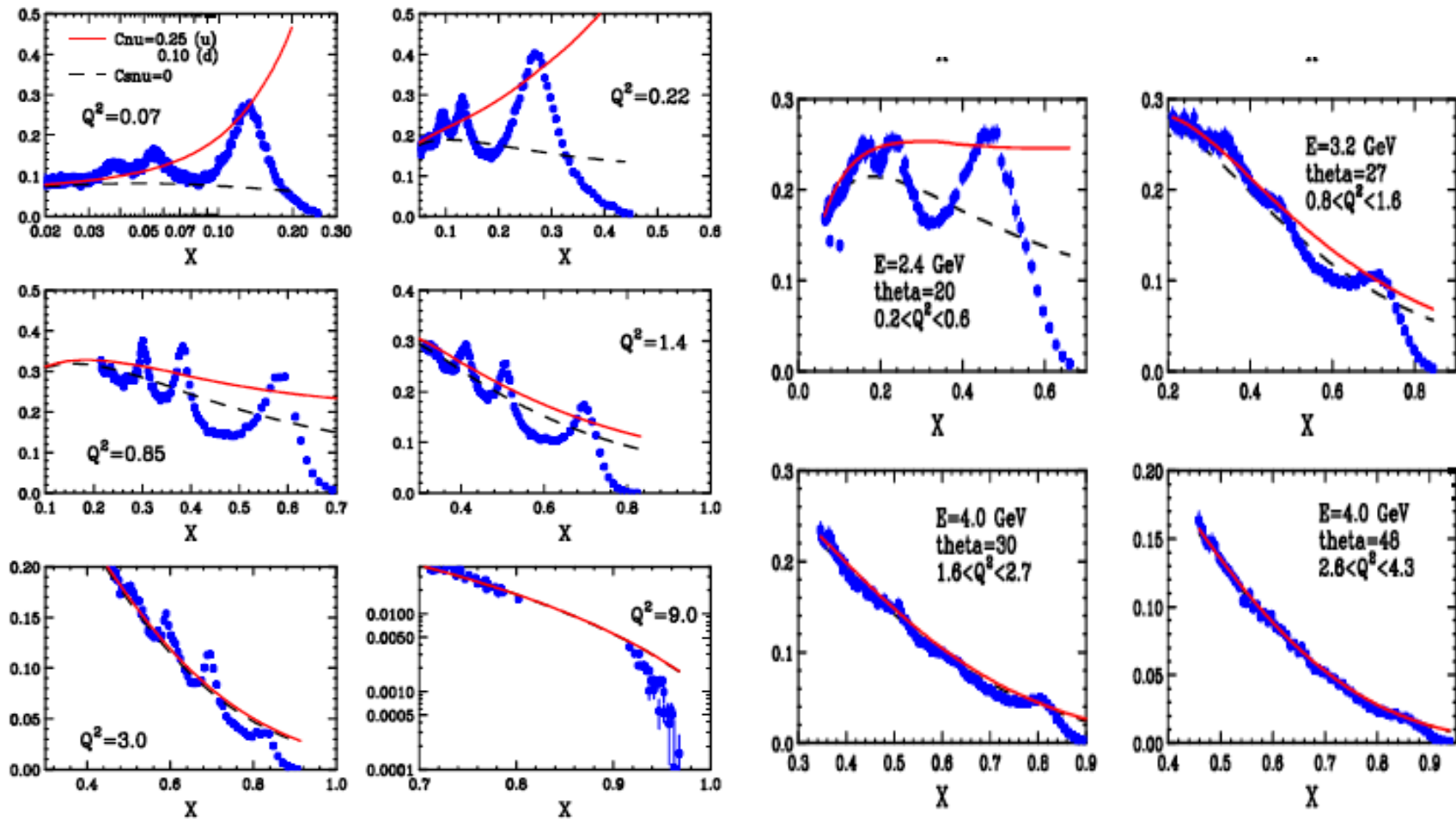
All scattering is from quarks. However, at low W , final state interaction between the quarks results in nucleon resonances. So nucleon resonance production may be thought of as one of the fragmentation products of the final state quarks .

Elastic electron scattering (quasielastic neutrino scattering), can be thought of an extreme case of FSI where the final state interaction leads to a single nucleon.

So if quark hadron duality works, PDFs can be used to predict the average structure function in the resonance region. Structure functions are just PDFs, modulated by a final state interaction which in the resonance region yields nucleon resonances, and in the DIS region yields a jet of hadrons.

Quark hadron duality (using the Nachtmann scaling variable) was found to work in electron scattering for $Q^2 > 1 \text{ GeV}^2$, even in the region of the Δ and quasielastic peak.

Questions: (1) What about lower Q^2
(2) What about neutrino scattering.



SLAC and Jlab data in the resonance region -- Quark Hadron Duality.

Works for $W > 1.5$ GeV (above delta resonance). Red curve = Bodek-Yang

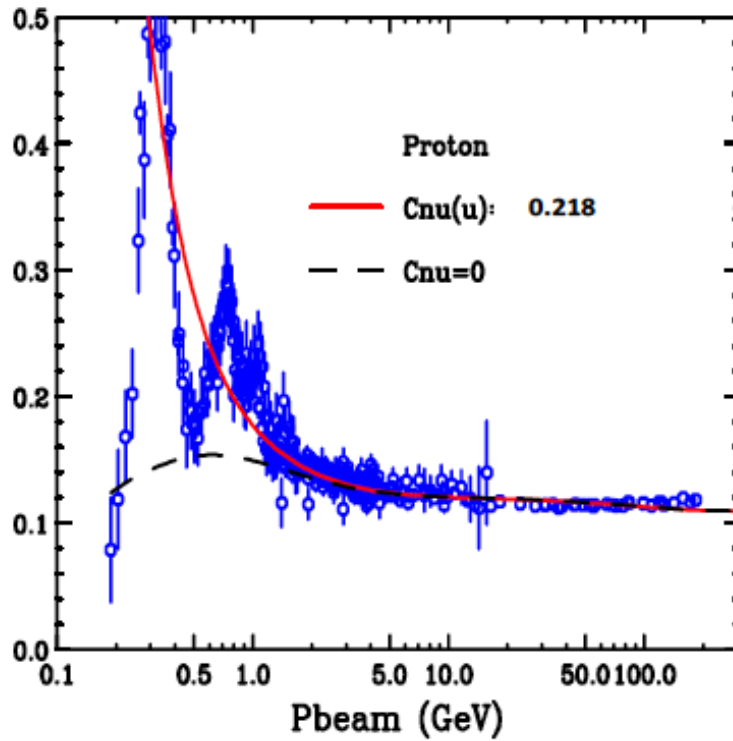
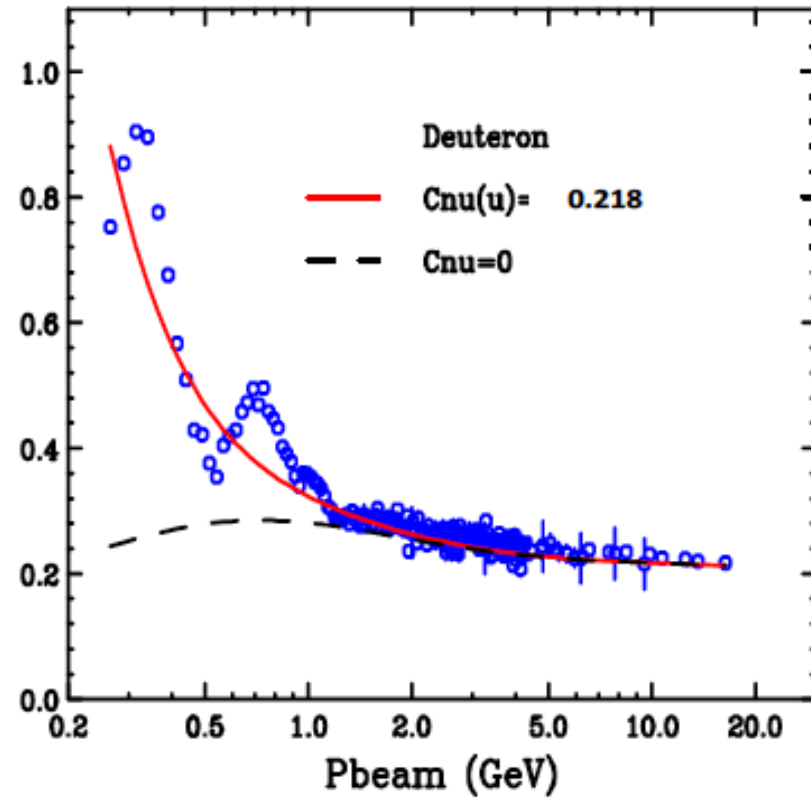


Photo-production for H and D, $Q^2=0$

$$\sigma(\gamma p) = \frac{4\pi^2\alpha}{Q^2} F_2^{e/\mu}(x, Q^2)$$

$$= \frac{0.112 \text{ mb}}{Q^2} F_2^{e/\mu}(x, Q^2)$$



Neutrinos and CVC

- CVC relates vector structure functions measured in electron scattering to vector structure functions in neutrino scattering. For quarks ($l=1/2$), PDFs are weighted by the square of the charges for electron scattering and the axial and vector weak couplings are equal.
- For quasielastic scattering, where there are anomalous magnetic moment we get a somewhat different relations between electron and neutrino form factors.
- For Δ production, $l=3/2$, we get another different relations between electron and neutrino form factors.
- Quark Hadron duality, for neutrinos, would work when we have several $l=1/2$ and $l=3/2$ resonances which interfere with each other such that the CVC relations for quarks are valid.

$W < 1.5 \text{ GeV}$

Why is QE and $\Delta^+ \Delta^- \Delta^0 \Delta^{++}$ (1236) special

$e + P \rightarrow e + P$ (QE) $l=1/2$ and
 $e + \Delta^+(1236)$ (resonance) $l=3/2$
 $e + N \rightarrow e + N$ (QE) $l=1/2$ and
 $e + \Delta^0(1236)$ (resonance) $l=3/2$

=====

$\nu + P \rightarrow$ no QE charged current process

only $\mu^- + \Delta^{++}(1236)$ (resonance) $l=3/2$
 $\nu + N \rightarrow \mu^- + p$ (QE) $l=1/2$ and
 $\mu^- + \Delta^+(1236)$ (resonance) $l=3/2$

=====

Anti $\nu + P \rightarrow \mu^+ + N$ (QE) $l=1/2$
 $\mu^+ + \Delta^0(1236)$ (resonance) $l=3/2$

Anti $\nu + N \rightarrow$ **no QE charged current process**
only $\mu^+ + \Delta^0(1236)$ (resonance) $l=1/2$

To have a chance for some form of quark-hadron duality to work.

one needs to average over both QE and Δ production

And/ or sum up neutron and proton processes

And/or sum up neutrinos and antineutrino structure functions.

But we want to describe all of these processes separately.

The picture of transition form factors

- Another way to look at resonance production is via transition form factors.
- When we have many resonances, PDFs should describe the average cross section.
- When we have few resonances, we need to use form factors and appropriate CVC relations between electron and neutrino scattering. (ie. QE and Δ).
- Above the Δ , we expect duality to begin to work better for 2nd (1512) resonance region. We expect duality to work much better by the time we get $W=1.7$ GeV resonance region.

Now to Neutrinos

Axial structure functions and form factors

11.1 Bodek-Yang Model Type I

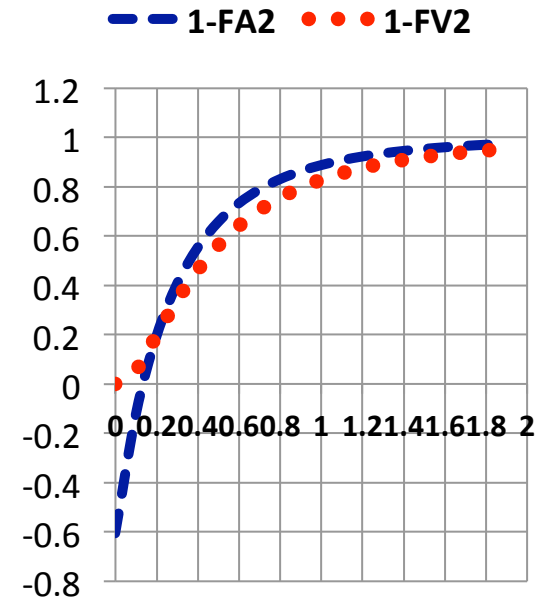
The first variation of our model (which we refer to as type I) assumes that the vector and axial components of the structure function \mathcal{F}_2^ν are equal at all values of Q^2 . i.e.

$$\mathcal{F}_2^{\nu-axial}(x, Q^2) = \mathcal{F}_2^{\nu-vector}(x, Q^2) \text{ (type I)}$$

11.2 Bodek-Yang model Type II

In the second variation of our model we account for the fact that the axial and vector structure functions are not equal at $Q^2=0$ as follows:

$$\begin{aligned} \mathcal{F}_2^{\nu-axial}(x, Q^2) = & \Sigma_i K_i^{axial}(Q^2) \xi_w q_i(\xi_w, Q^2) \\ & + \Sigma_j K_j^{axial}(Q^2) \xi_w \bar{q}_j(\xi_w, Q^2) \end{aligned}$$



Type II model, not implemented in neutrino MC's

11.2.1 Axial sea

For sea quarks, use use the same axial K factor for all types of quarks.

$$K_{sea}^{axial}(Q^2) = \frac{Q^2 + P_{sea}^{axial}}{Q^2 + C_{sea}^{axial}}$$

We refer to the non-zero value of the K_{sea}^{axial} at $Q^2=0$ as the PCAC term in \mathcal{F}_2 . We use $P_{sea}^{axial} = 0.018 \pm 0.09$, and $C_{sea}^{axial} = 0.3$. With the above values we get:

$$K_{sea}^{axial}(Q^2) = \frac{Q^2 + 0.018 \pm 0.09}{Q^2 + 0.3}$$

which implies that the axial K factor for the sea at $Q^2 = 0$ is 0.06. The axial sea parameters are extracted from low Q^2 CCFR and CHORUS data, and from PCAC consider-

So at $Q^2=0$, the vector structure functions for the sea are zero and the axial structure functions for the sea are 6% of their value at $Q^2 = 1 \text{ GeV}^2$

11.2.2 Axial valence

For the valence quarks, we note that the following is a good approximation to the vector K factor for valence quarks.

$$K_{valence}^{vector}(Q^2) \approx [1 - G_D^2(Q^2)] \approx \frac{Q^2}{Q^2 + 0.18}$$

We use a similar form for the axial K factor for valence quarks.

$$K_{valence}^{axial}(Q^2) = \frac{Q^2 + P_{valence}^{axial}}{Q^2 + 0.18} \quad (type II)$$

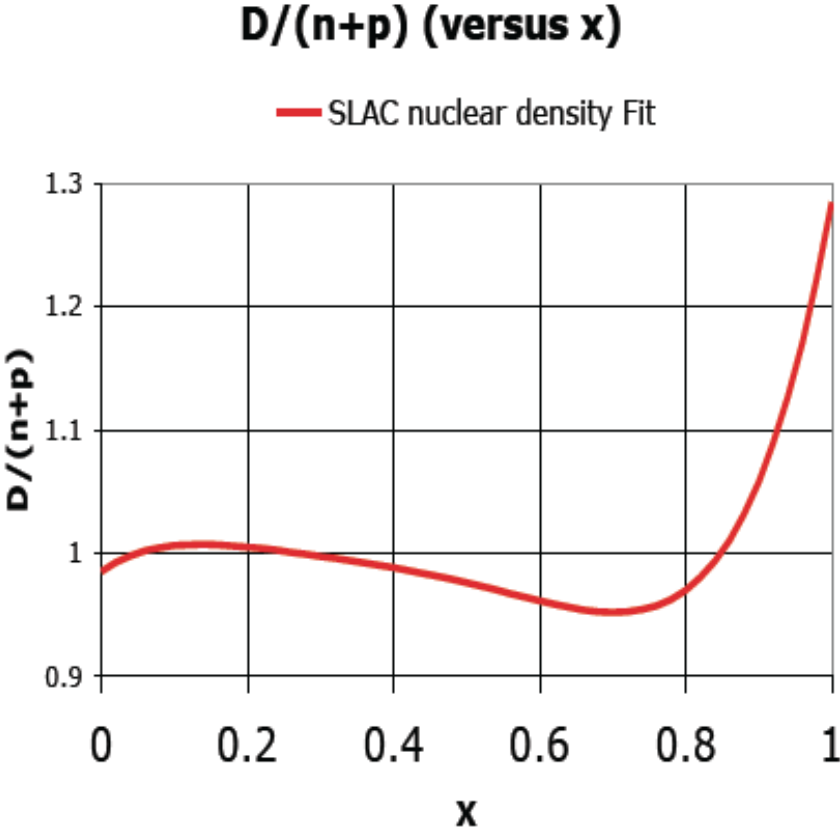
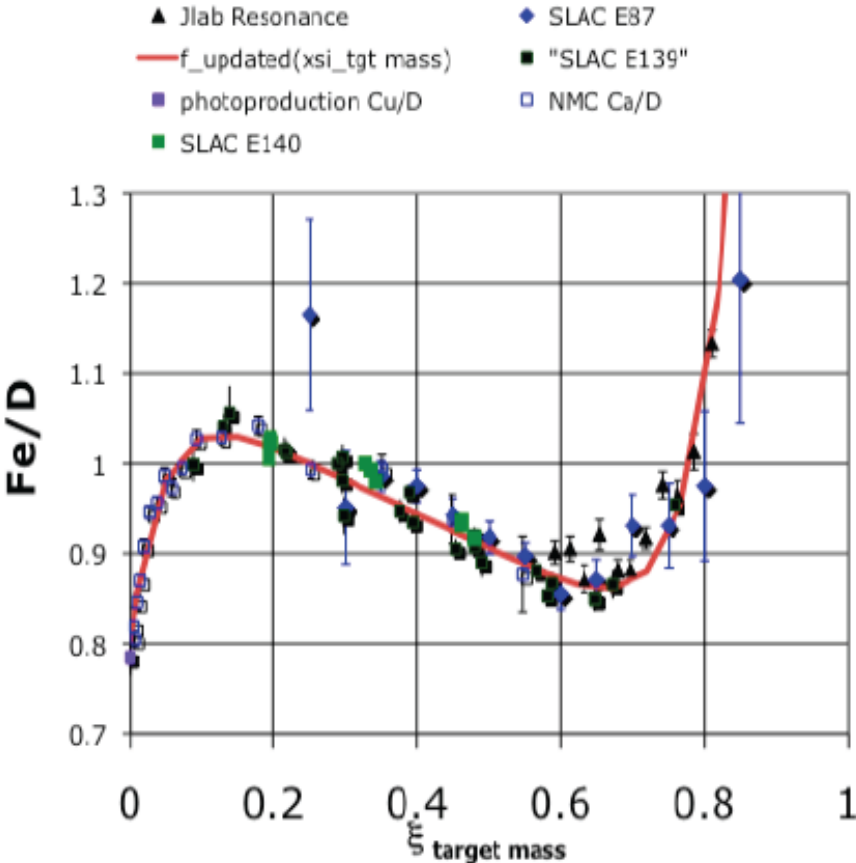
Where $P_{valence}^{axial} = 0.018 \pm 0.09$ is chosen to get agreement with measured high energy neutrino and antineutrino total cross sections. Therefore,

$$K_{valence}^{axial}(Q^2) = \frac{Q^2 + 0.018 \pm 0.09}{Q^2 + 0.18} \quad (type II)$$

So at $Q^2=0$, the vector structure functions for the valence quarks are zero and the axial structure functions for the valence quarks are 10% of their value at $Q^2 = 1 \text{ GeV}^2$

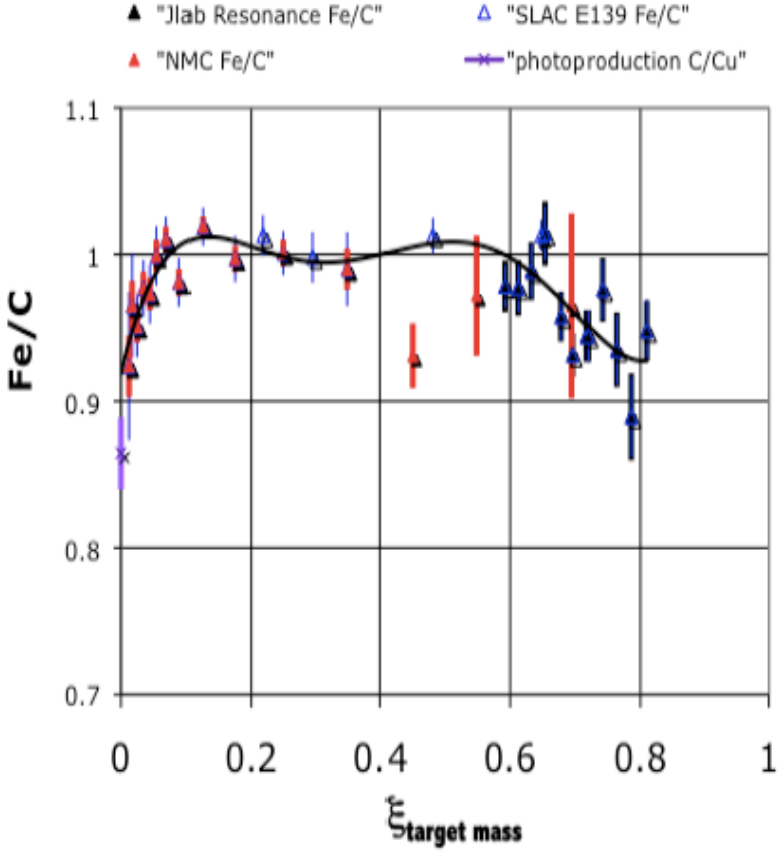
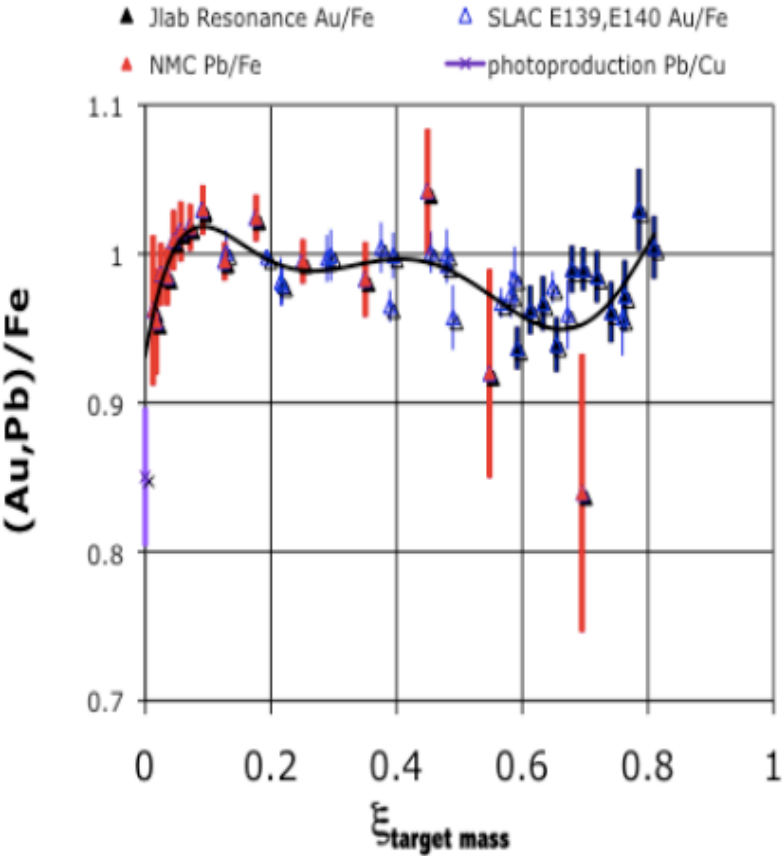
EMC Effect Corrections in Fe to compare to Fe CCFR/NuTeV/CDHS Data

10 A. Bodek and Un-ki Yang: Axial and Vector Structure Functions for Electron- and Neutrino- Nucleon Scattering



EMC Effect Corrections in Pb to compare to Fe CCFR/NuTeV/CDHS Data

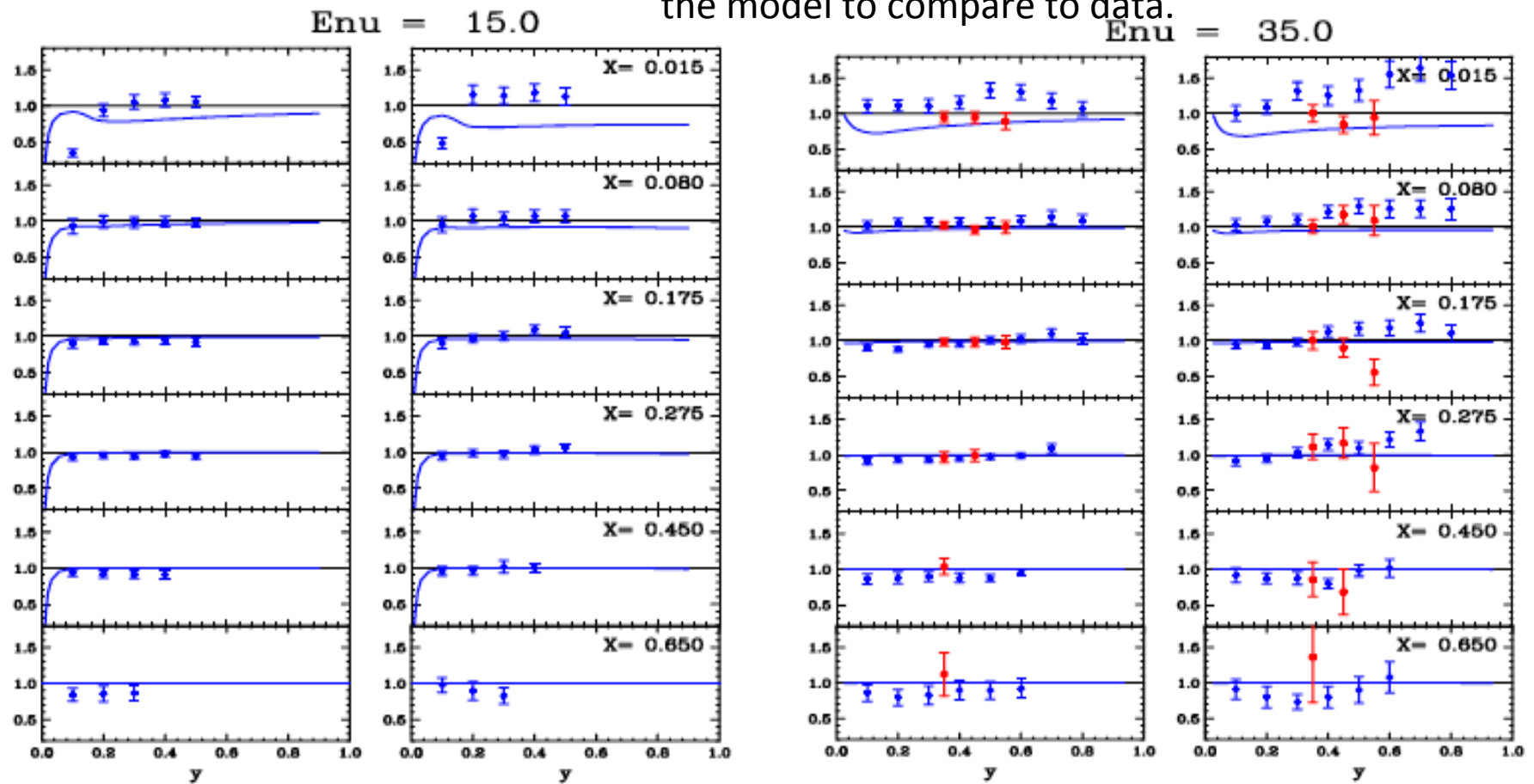
A. Bodek and Un-ki Yang: Axial and Vector Structure Functions for Electron- and Neutrino- Nucleon Scattering



Corrections is **larger** in Pb (CHORUS) than in iron especially in shadowing region (low x) Corrections is smaller in Carbon than in iron

Testing the axial structure functions

Note: Here, radiative corrections were applied to the model to compare to data.



$d^2\sigma/dx dy$ ratio of neutrino data to Bodek-Yang with PCAC axial at low x .

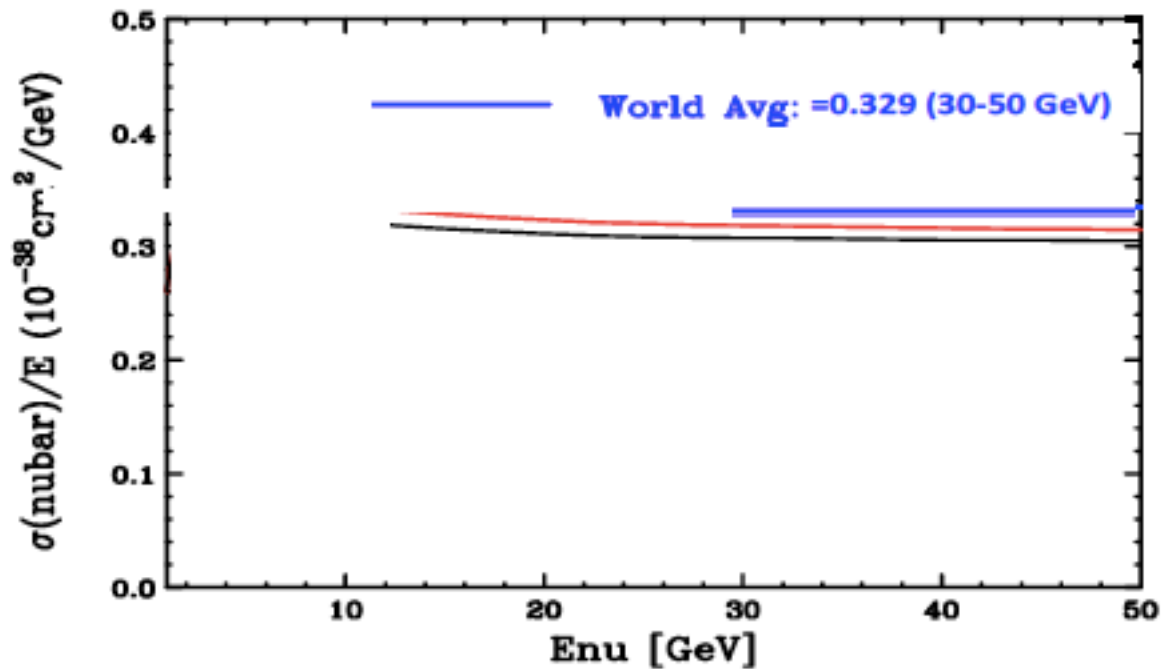
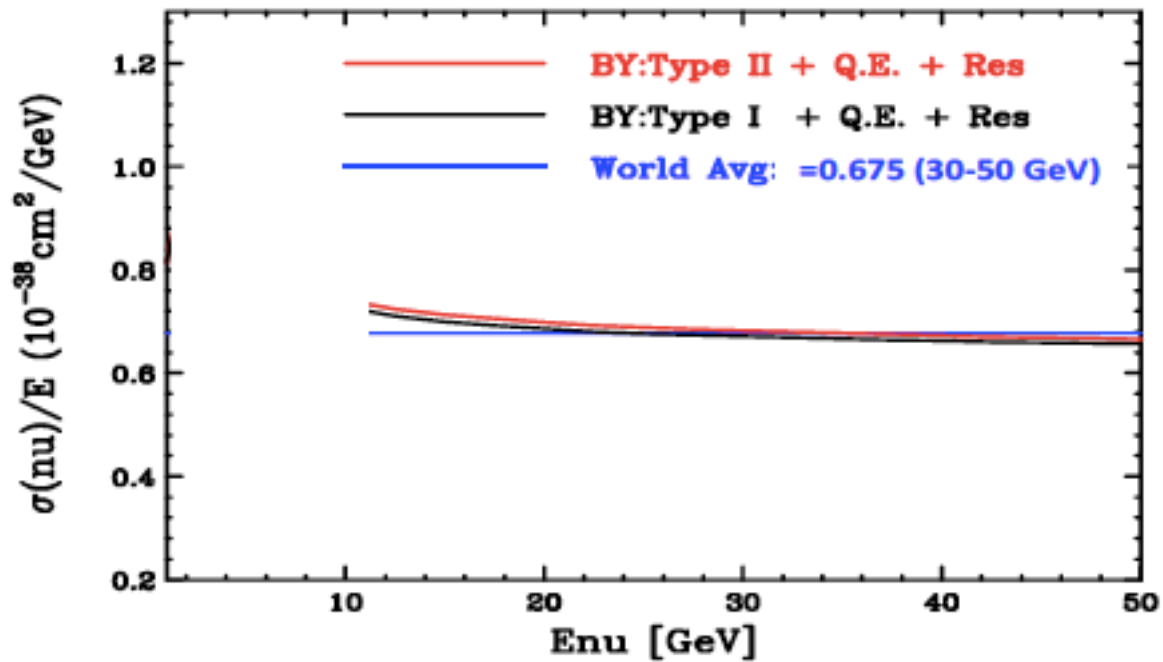
CHORUS (Pb) – Blue. CCFR (Fe) – red (neutrinos left, antineutrinos right)

Ratio to Bodek-Yang model including axial contribution from PCAC (Blue line is if we assume $V=A$).

These data are in the continuum. Nuclear corrections applied from electron scattering. Similar plots will be available from MINERvA for lower energies (on Carbon) including the resonance region.

Nuclear Corrections

- At low x , either shadowing for the axial current is



Here, we use Bodek Yang above $W=1.4$ GeV, and use GENIE below $W=1.4$ GeV

=====
 Understanding of Resonance region needs to be improved.

Understanding of axial vs vector and nuclear effects needs to be improved.

We are now accumulating data with MINERvA for this purpose.

Table 3. Sources of systematic error in the predicted inelastic contribution to the total cross section on iron (for $W > 1.8\text{GeV}$). The change (positive or negative) in the neutrino, antineutrino and the $\sigma_{\bar{\nu}}/\sigma_{\nu}$ ratio that originate from a plus one standard deviation change in the ratio of transverse to longitudinal structure functions (R), the fraction of antiquarks ($f_{\bar{q}}$), the axial quark-antiquark sea, and the overall normalization of the structure functions (N).

source	change (error)	change in σ_{ν}	change in $\sigma_{\bar{\nu}}$	change in $\sigma_{\bar{\nu}}/\sigma_{\nu}$
R	+0.05	-1.0%	-2.0%	-1%
$f_{\bar{q}}$	+5%	-0.7%	+1.4%	+2.1%
P (K^{axial})	+ 50%	+1.3%	+1.9%	+1.2%
N	+3%	+3%	+3%	0
Total		$\pm 3.4\%$	$\pm 4.3\%$	$\pm 2.5\%$

The above is only for the $W > 1.8\text{ GeV}$ contribution to the neutrino cross section. Modeling of the axial structure functions should be validated with future neutrino data.

The modeling in the resonance region is in a much more primitive stage and can be greatly improved. As a first step, the vector structure functions need to be validated against existing electron scattering data in the resonance region. There is a lot of work to be done.

Scattering from Nucleons Bound in nuclei is more complicated (nuclear effects)

1. Scattering is smeared by Fermi motion (important at large x)
2. Internal structure of nucleons modified by medium (e.g. EMC effect)
3. Nucleons can shadow each other at low Q^2 (inelastic, small X).

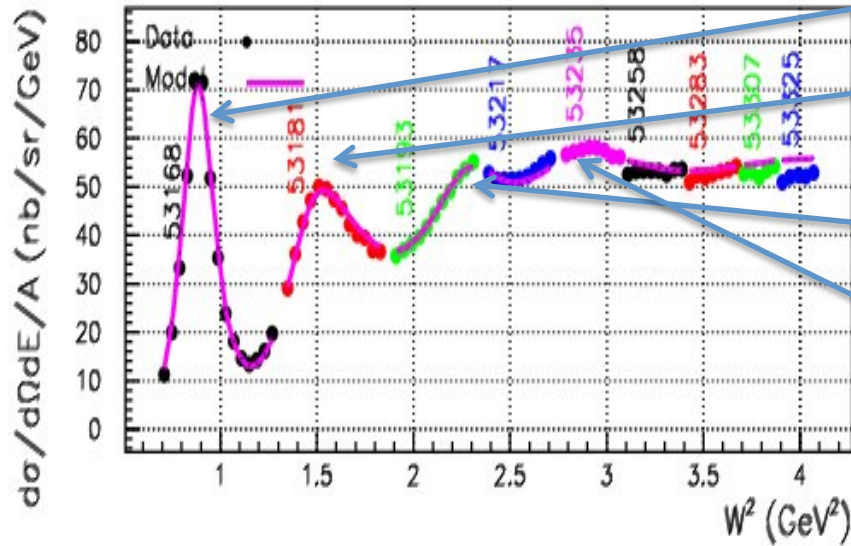
And for Quasielastic/Delta production there are additional effects:

1. For QE and Delta production at very low Q^2 there should be Pauli suppression since the final state cannot occupy the same state as the other nucleons. ($Q^2 < 0.1 \text{ GeV}^2$) and RPA effects (breakdown of impulse approximation)
2. For Quasielastic transverse scattering (magnetic) there can be scattering from additional currents in the nucleus (e.g. Meson Exchange Currents, Transverse enhancement).

Electron scattering data can be used to study all of these nuclear effects, with the caveat that some of the effects may be different for the axial current.

1. Scattering is smeared by Fermi motion (important at large x)

Target=D2, Ebeam=2.3 GeV, $\theta=30$



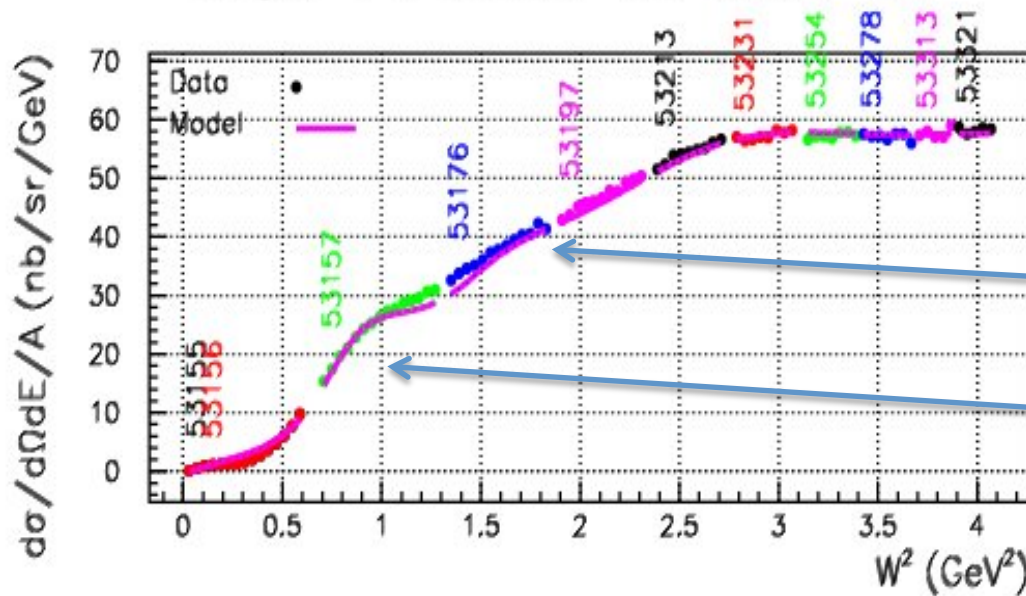
Deuterium: Higher Q^2
QE peak some smearing.

Δ 1236 resonance
some smearing

1512 resonance is
a sum of several
resonances and
continuum

Third resonance is a sum
of more resonances and
continuum

Target=Fe, Ebeam=2.3 GeV, $\theta=30$



Same data on Iron:

Fermi motion in iron is larger than
in Deuterium

smearing of resonances
smearing of QE peaks

Effect of Fermi motion is very Q^2
dependent

2. Internal structure of nucleons modified by medium (e.g. EMC effect)
3. Nucleons can shadow and anti-shadow each other at low Q^2 (inelastic, small X).

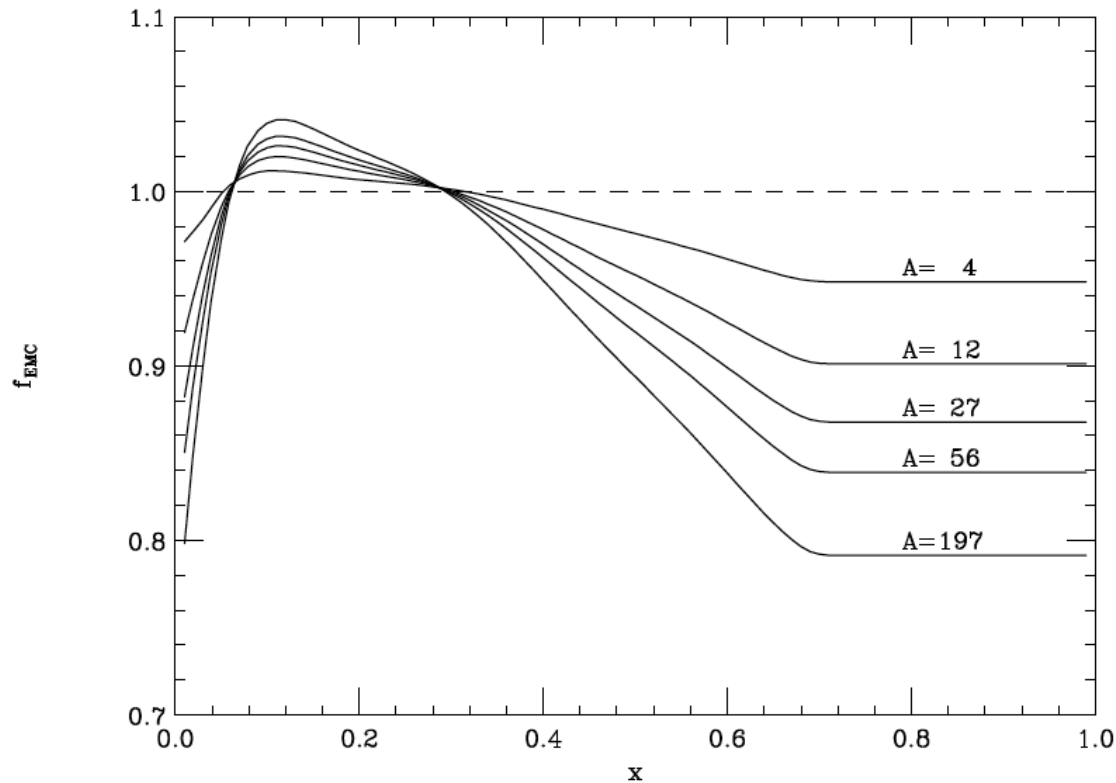


FIG. 1: Illustration of the x -dependence of the function f_{EMC} for five values of atomic number A .

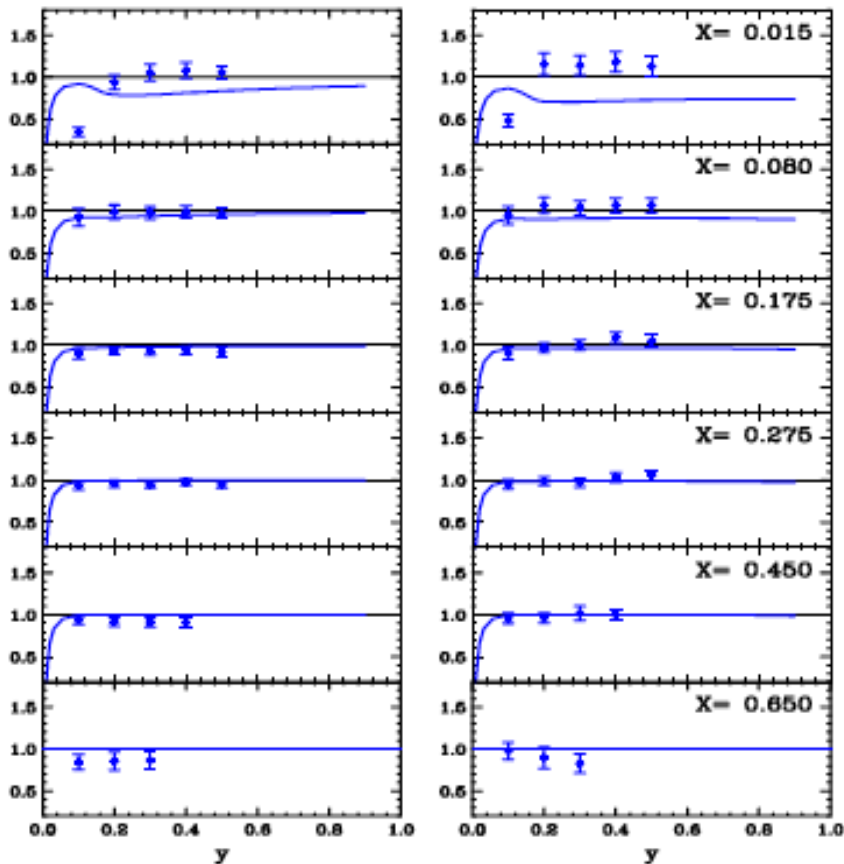
EMC effect and shadowing parametrization from DIS e scattering data at SLAC (higher Q^2 data in the DIS region. Currently, it is also used in resonance region and at low Q^2

We we will use Jlab JUPITER data to investigate these nuclear effects at low Q^2 and in the resonance region. And we have have similar data from MINERvA

Where do we go from here

Neutrino cross sections should be published as $d^2\sigma/dx dy$

$E_{\nu} = 15.0$



We are accumulating data for neutrino differential on neutrino double differential cross sections, which include both vector and axial contributions to the structure functions

We should look at similar data for electron scattering (from Jlab) for the same nuclear targets to determine the vector structure functions for the nuclear targets.

Structure functions can be parametrized in terms of effective leading order PDFs, or in terms of transition form factors for a multitude of resonances.

When we have many resonances, effective leading order PDFs are a good way to understand the data even in the resonance region.

Additional Slides

Three comments on QE scattering

A. Bodek

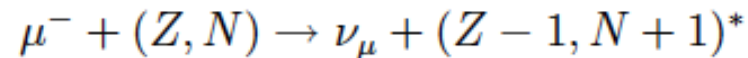
University of Rochester

1. Nuclear effects in Muon Capture

Muon capture on nuclei with $N > Z$, random phase approximation, and in-medium renormalization of the axial vector coupling constant

E. Kolbe (Basel U.), K. Langanke (Aarhus U.), P. Vogel (Caltech). Jun 2000. 9 pp.
Published in Phys.Rev. C62 (2000) 055502 e-Print: nucl-th/0006007 |

The capture of a negative muon from the atomic $1s$ orbit,



The nuclear response in muon capture is governed by the momentum transfer which is of the order of the muon mass. The energy transferred to the nucleus is restricted from below by the mass difference of the initial and final nuclei, and from above by the muon mass.

We use the random phase approximation to describe the muon capture rate on ^{44}Ca , ^{48}Ca , ^{56}Fe , ^{90}Zr , and ^{208}Pb . With ^{40}Ca as a test case, we show that the Continuum Random Phase Approximation (CRPA) and the standard RPA give essentially equivalent descriptions of the muon capture process. Using the standard RPA with the free nucleon weak form factors we reproduce the experimental total capture rates on these nuclei quite well. Confirming our previous CRPA result for the $N = Z$ nuclei, we find that the calculated rates would be significantly lower than the data if the in-medium quenching of the axial-vector coupling constant were employed.

TABLES

TABLE I. μ^- -capture rates calculated within the standard (SRPA) and continuum (CRPA) models in units of $10^3/s$. The radius r and diffuseness d of the extended nuclear charge distribution were set to $(r, d) = (1.07 \text{ fm}, 0.50 \text{ fm})$ for ^{12}C and $(r, d) = (1.07 \text{ fm}, 0.57 \text{ fm})$ for all other nuclei. The Landau-Migdal force (LM) is used throughout.

nucleus	Exp. [3]	SRPA	SRPA	CRPA(LM)	CRPA(LM)
		$g_A(0) = 1.26$	$g_A(0) = 1.0$	$g_A(0) = 1.26$	$g_A(0) = 1.0$
^{12}C	32.8 ± 0.8	→		$31.3^{(3)}$	$22.9^{(3)}$
^{16}O	102.6 ± 0.6	→		103.2	75.8
^{40}Ca	$2544 \pm 7^{(1)}$	2547	1846	2489	1800
^{44}Ca	1793 ± 40	1722	1238		
^{48}Ca	$1164^{(2)}$	1301	930		
^{56}Fe	4400 ± 100	$4460^{(3)}$	$3430^{(3)}$		
^{90}Zr	9350 ± 100	10288	7400		
^{208}Pb	13450 ± 180	16057	11436		

⁽¹⁾ Corrected from the data for natural Ca

⁽²⁾ Extrapolated using the Primakoff formula fitted to ^{40}Ca and ^{44}Ca

⁽³⁾ Calculated with partial occupation of the single particle subshells, see [17].

In conclusion, the present analysis shows that the CRPA and SRPA methods are capable of describing the total μ^- capture rates quite well in a large range of nuclei. The dependence of the muon capture rate on the isospin, the so-called Primakoff rule [16], is also reasonably well reproduced. There is no indication of the necessity to apply any quenching to the operators responsible for the μ^- process. Thus our findings indicate that any in-medium quenching of the axial current matrix elements appears to be restricted to the $0\hbar\omega$ spin changing operators, i.e. to the Gamow-Teller operator.

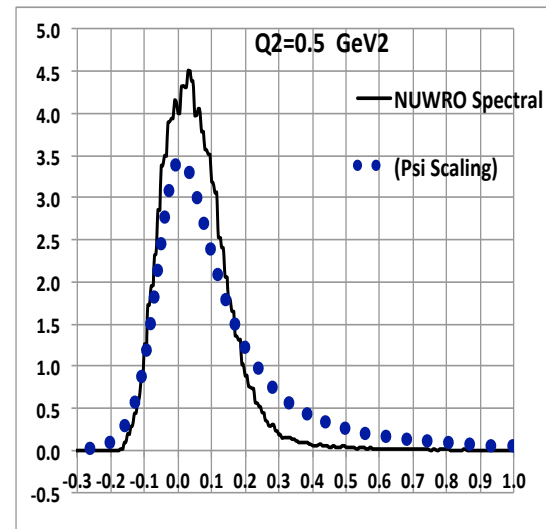
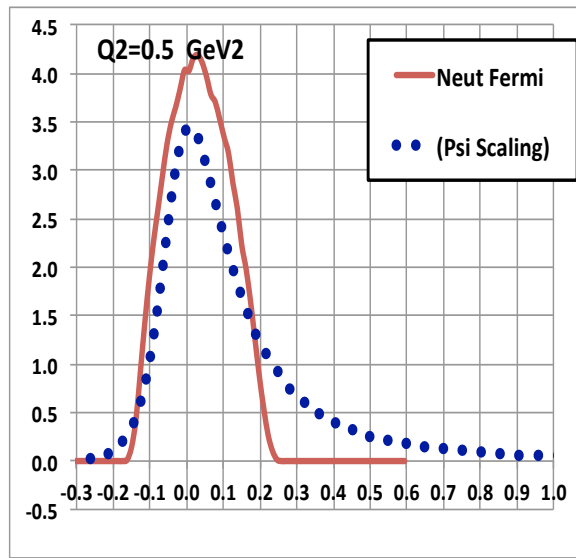
Therefore: At low Q^2 , the data indicates that the axial coupling for nucleons bound in nuclei is the same as for free nucleons.

2 comments on QE Scattering.

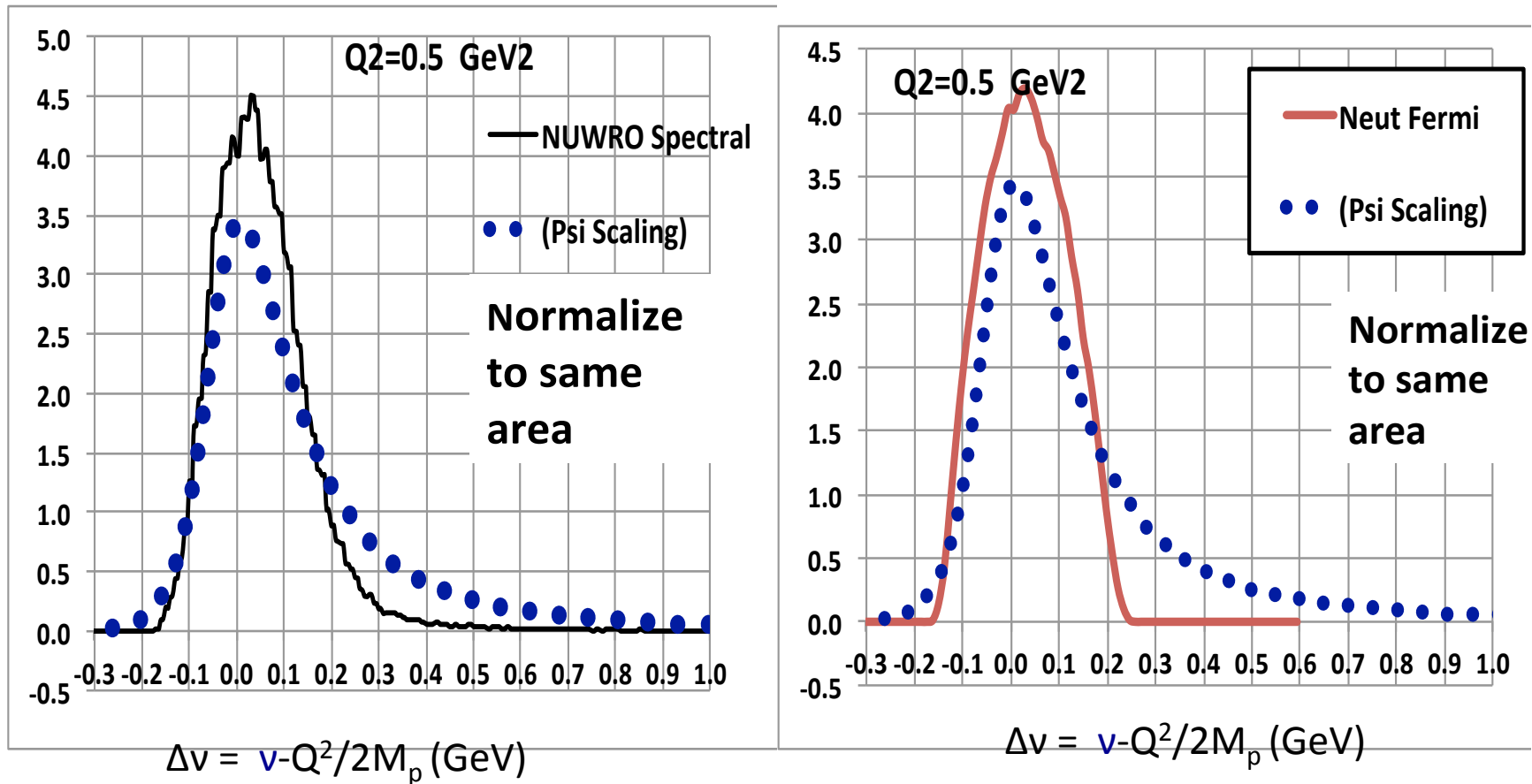
The current analyses of neutrino oscillations and $d\sigma/dQ^2$ neglect two effects which result in a migration of QE events to lower reconstructed neutrino.

2. Radiative corrections (internal Brem photon emission) by the muon leg in the scattering process. Note that these are applied in electron scattering. Unlike external Brem, internal Brem is logarithmic in lepton mass. \rightarrow help from theorists would be much appreciated here.

3, The Ψ' scaling has long tail in QE scattering the is extracted from the longitudinal response in electron scattering data. One should compare differential distribution to Ψ' -scaling + (MEC or TE).



Comparison of Spectral function calculations to Psi scaling fits to electron scattering data



If we compare the shape of the QE peak at fixed Q^2 , we should get the same shape in electron scattering and neutrino scattering.

The Psi' scaling curve has a larger tail than the Fermi Gas nor Benhar Fantoni spectral for QE scattering. This difference needs to be understood.

(Increasing the high momentum components in the Spectral Function would reduce some of the difference).

Longitudinal vs Transverse

(Scattering from Quarks, structure function description)

- Transverse means polarization of the electric field perpendicular to the direction of motion. i.e. the spin/helicity is along the the direction of motion (e.g. real photons). Since quarks are very low mass, they have +-helicity. Therefore, the absorption of transverse photons results in spin/helicity flip of the quarks (which is the dominant process).
- Longitudinal means that the spin is perpendicular to the direction of motion. This is only possible for off-shell virtual photons. This means that the photons can only be absorbed by quarks which have a transverse momentum (e.g. from gluon emission), or binding the nucleon (target mass).
- For charged current scattering from quarks: vector=axial

Longitudinal vs Transverse

(For Quasielastic and Resonance Excitation – form factor discription)

- Transverse cross section is from the MAGNETIC moment distribution in the nucleon (magnetic form factor)
- Longitudinal cross section is on ELECTRIC CHARGE distribution in the nucleon (electric form factor).